
THE S2 HIERARCHICAL DISCRETE GLOBAL GRID AS A NEXUS FOR DATA REPRESENTATION, INTEGRATION, AND QUERYING ACROSS GEOSPATIAL KNOWLEDGE GRAPHS

A PREPRINT

Shirly Stephen
NCEAS | Department of Geography
University of California
Santa Barbara, CA, USA
shirlystephen@ucsb.edu

Mitchell Faulk
NCEAS, University of California
Santa Barbara, CA, USA

Krzysztof Janowicz
Geoinformatics, University of Vienna
Vienna, Austria

Colby Fisher
Hydronos Labs
New Jersey, USA

Thomas Thelen
NCEAS, University of California
Santa Barbara, CA, USA

Rui Zhu
School of Geographical Sciences
University of Bristol, Bristol, UK

Pascal Hitzler
Department of Computer Science
Kansas State University, Kansas, USA

Cogan Shimizu
Department of Computer Science & Engineering
Wright State University, Ohio, USA

Kitty Currier
Department of Geography
University of California, Santa Barbara
California, USA

Mark Schildhauer
NCEAS
University of California, Santa Barbara
California, USA

Dean Rehberger
Department of History
Michigan State University, MI, USA

Zhangyu Wang
Department of Geography
University of California, Santa Barbara
California, USA

Antrea Christou
Department of Computer Science & Engineering
Wright State University, Ohio, USA
Santa Barbara
California, USA

October 22, 2024

ABSTRACT

Geospatial Knowledge Graphs (GeoKGs) have become integral to the growing field of Geospatial Artificial Intelligence. Initiatives like the U.S. National Science Foundation's Open Knowledge Network program aim to create an ecosystem of nation-scale, cross-disciplinary GeoKGs that provide AI-ready geospatial data aligned with FAIR principles. However, building this infrastructure presents key challenges, including 1) managing large volumes of data, 2) the computational complexity of discovering topological relations via SPARQL, and 3) conflating multi-scale raster and vector data. Discrete Global Grid Systems (DGGs) help tackle these issues by offering efficient data integration and representation strategies. The KnowWhereGraph utilizes Google's S2 Geometry — a DGGs

framework — to enable efficient multi-source data processing, qualitative spatial querying, and cross-graph integration. This paper outlines the implementation of S2 within KnowWhereGraph, emphasizing its role in topologically enriching and semantically compressing data. Ultimately, this work demonstrates the potential of DGGs frameworks, particularly S2, for building scalable GeoKGs.

Keywords geospatial knowledge graphs · discrete global grid systems · S2 geometry · linked data · query optimization · spatial ontologies · spatial data integration

1 Introduction

Knowledge Graphs (KGs), originating from Semantic Web research [Hitzler, 2021], have revolutionized the data science landscape by facilitating the integration and enrichment of vast, multi-source, and heterogeneous data while empowering AI applications to deliver high-quality, trusted insights for scientific decision-making [Ji et al., 2021, Abu-Salih, 2021]. To support translational research — bridging the gap between fundamental research and real-world applications — initiatives like the U.S. National Science Foundation’s Open Knowledge Network (OKN) program¹ and the Linked Open Data (LOD) Cloud² are driving the development of comprehensive ecosystems of nation-scale KGs that adhere to FAIR (Findable, Accessible, Interoperable, Reusable) data principles [Wilkinson et al., 2016]. These initiatives aim to create data-centric infrastructures for addressing complex cross-disciplinary challenges, ranging from climate change to economic equity. A central theme interlinking the various domain KGs in these infrastructures is the geospatial layer comprised of Geospatial Knowledge Graphs (GeoKGs), such as the KnowWhereGraph [Janowicz et al., 2022] and Urban Flooding Open Knowledge Network (UF-OKN) [Johnson et al., 2022]. GeoKGs are now a critical component of modern Geospatial Artificial Intelligence (GeoAI), providing a structured and interconnected approach to managing and analyzing extensive spatial datasets from heterogeneous sources [Janowicz et al., 2022, Yan et al., 2020]. The Resource Description Framework (RDF) [Manola et al., 2004] is the widely adopted paradigm for GeoKGs due to its semantic richness, high interoperability, and adherence to open standards. Additionally, the Open Geospatial Consortium’s (OGC) GeoSPARQL standard [Car and Homburg, 2022] enhances the representation of spatial information in RDF, enabling quantitative and qualitative spatial querying. This capability of GeoKGs is leveraged in AI systems to provide more intelligent, multi-faceted, and context-aware services [Janowicz et al., 2023].

Despite the promise of GeoKGs, three primary challenges impede their effective implementation: handling and storing immense volumes of (geospatial) data, the computational complexity involved in large-scale spatial querying, and analyzing raster and vector data together at various spatial scales. Graph databases capable of managing large datasets (e.g., Neptune, Neo4j) lack any GeoSPARQL support. GeoSPARQL-compliant RDF databases [Jovanovik et al., 2021] like Blazegraph³, GraphDB⁴, Virtuoso⁵, and Stardog⁶ use indexing methods such as R-trees, quadtrees, and geohashing. However, these methods are not optimized for cross-scale analyses, global datasets, and dense graphs with high degrees of spatial overlap [Huang et al., 2019, Theocharidis et al., 2019]. High memory costs from building and maintaining extensive indexes, computational costs of traversing deep R-trees and quadtrees [Kothuri et al., 2002], and inefficiencies in proximity searches due to boundary ambiguities in geohashing [Acharya, 2023] are just some challenges with large graphs. While these indexing methods can accelerate fundamental spatial filtering queries such as point-based queries, containment queries, and spatial joins for range and nearest-neighbor queries, complex queries involving spatial refinements, such as polygon intersection, spatial cross-matching, and identifying spatial patterns, remain highly expensive. For example, queries like “*Find the regions where earthquakes occurred in 2023*” or “*Find comparable areas that are earthquake-prone*” require a large number of spatial joins to determine relevancy, and can be inefficient or even return incorrect results [Huang et al., 2019]. Experimental evaluations show that topological computation becomes highly expensive or nearly intractable in GeoKGs characterized by extensive data volume, uneven data scale, and diverse categories of data [Theocharidis et al., 2019, Li et al., 2022a]. Furthermore, the qualitative spatial functions that GeoSPARQL provides are insufficient for multi-scale analytics [Manley, 2021]. For instance, conflating a vector region dataset with a map scale of 1:50,000 alongside a land-use raster dataset of 30 m resolution can be problematic [Davis et al., 1991]. Addressing these challenges requires innovative data integration and management strategies that can efficiently handle large, multi-scale, multi-format geospatial data and support complex topological queries in the context of GeoKGs.

¹<https://www.proto-okn.net/>

²<https://lod-cloud.net/>

³<https://blazegraph.com/>

⁴<https://graphdb.ontotext.com/>

⁵<https://virtuoso.openlinksw.com/>

⁶<https://www.stardog.com/>

Discrete Global Grid Systems (DGGS) are spatial indexing frameworks that tessellate the Earth’s surface into hierarchical, regular grids [Sahr et al., 2003]. Unlike traditional GIS systems that use latitude and longitude coordinates, a DGGS employs cell identifiers (cell IDs) to uniquely reference discrete portions of the Earth’s surface. DGGS frameworks have been utilized in geospatial applications since the early 1990s [Goodchild, 1994], but have more recently emerged as a key technology for next-generation GIS [Li and Stefanakis, 2020, Hojati et al., 2022, Bondaruk et al., 2020] and Digital Earth systems [Mahdavi-Amiri et al., 2015, Robertson et al., 2020, Yao et al., 2019, Hojati et al., 2022]. This is primarily driven by the standardization of DGGS configurations by the OGC in 2017 [OGC, 2017] that spurred the proliferation of DGGS implementations and their open-source software libraries, such as Google’s S2 Geometry [Veach et al., 2017], Uber’s H3 [Uber, 2023], rHEalPIX [Gibb, 2016], and OpenEAGGR [Riskaware Ltd, 2017]. These libraries provide (quantization) functions to assign geometries to cells, and spatial operations for cell navigation [Li and Stefanakis, 2020]. Their algorithms leverage cell IDs as well as their inherent inter-relations to replace complex spatial computations with simple coding operations, making DGGS frameworks powerful tools for efficient data integration, retrieval, and reduction of analytical complexity across various geospatial application domains [Li et al., 2021, Kranstauber et al., 2015, Romanov and Khvostov, 2018, Pereira et al., 2024, Lin et al., 2018]. A seminal paper by Goodchild in 2018 [Goodchild, 2018] highlighted the benefits of DGGS for multi-scale, multi-format data integration within linked data frameworks, sparking interest in the GeoKG and OKN communities [Bastrakova and Crossman, 2020]. Despite its potential, the adoption of DGGS in GeoKGs remains limited. One reason is the lack of support in graph databases for DGGS library interfaces or full support for gridded representations of geospatial data. While GeoSPARQL 1.1 [Car et al., 2023] introduces a generic format for DGGS geometry serialization [Car and Homburg, 2022], it does not yet provide the ability to interpret specific cell IDs according to the various DGGS frameworks available. Furthermore, testing this implementation in RDF databases is still in its early stages [Habgood et al., 2022]. Few graph databases support DGGS-based indexing, such as those using S2 and H3 (e.g., NebulaGraphDB), but these are not RDF-based or GeoSPARQL-compliant [Jovanovik et al., 2021]. The commercial Foursquare GeoKG [Gundeti, 2023] utilizes H3 for location-specific business use cases, but only as an indexing framework. More sophisticated usages of DGGS in GeoKGs, such as for spatial data compression through semantic compression have been postulated [Zalewski et al., 2021] but not practically explored until KnowWhereGraph.

The KnowWhereGraph (KWG) [Janowicz et al., 2022], a GeoKG within the OKN framework, employs the S2 Geometry to spatially integrate large-scale geospatial data by optimizing their storage, processing, visualization, and analysis across various data types, shapes, scales, and precision. KWG transforms siloed heterogeneous location and environmental observation data into actionable insights for environmental intelligence by *enhancing cross-domain data interoperability, contextualizing data, and generating AI-ready geospatial data*. Rather than relying on S2 as an implicit indexing method in GraphDB (the graph database where KWG is deployed), KWG represents S2 cells as a set of nodes within an S2-RDF graph. GeoSPARQL’s Dimensionally Extended 9-Intersection Model (DE-9IM) relations [Egenhofer et al., 1994] are employed to model cell navigation (parent, child, neighbor) and topological connections between S2 cells and other geographic features. Integrating S2 as a spatial reference framework within KWG provides a robust infrastructure that supports cross-domain data linkages and abstracts spatial analytics while fostering a rich environment for modeling and computation of geographical information.

This paper details this implementation by outlining the development of the S2-RDF Graph and describing the following two methods to quantize spatial data onto S2 cells.

1. *Topological enrichment of cells* involves materializing topological relations (based on DE-9IM) between S2 cells and geographic features having explicit geometries in the graph. This approach mitigates the tractability challenges of calculating these relationships at runtime via GeoSPARQL, even when utilizing efficient implicit spatial indexing methods.
2. *Grid-based data discretization* involves transforming non-DGGS data (both vector and raster) using techniques like statistical aggregation, decomposition, and spatial overlay to represent them as S2-cell-based gridded data. This process enables geometric simplification, scalable data representation, and integrated raster/vector analysis. In this framework, the S2 cells serve as the *spatial feature of interest* [Janowicz et al., 2019], linking various thematic observations.

The significant spatial computational capabilities of the S2 Geometry library [Veach et al., 2017] are utilized in a Python-based RDF processing environment to materialize statements for enrichment and discretization. Through topological enrichment, S2 cells are tagged with spatial features, thereby associating cells with observations linked to those features, e.g., S2 cells are linked to climate observations via topologically connected climate division features. Through discretization, S2 cells are enriched with temporally-scoped observations computed for the specific cell area, e.g., the area of a crop type within a cell. Once the S2 grid is augmented with each dataset using these methods, each cell node can be queried as a set of individual objects containing diverse pieces of information that can then be *spatially fused* or *conflated* for analysis. This approach is powerful because once a dataset is quantized on the S2 grid, it eliminates the need for repeated spatial analytics and related GIS processes to integrate and compare disparate datasets. Our experience indicates that leveraging S2 in KWG has enabled efficient multi-source data processing and faster

qualitative spatial querying while constructing an enriched GeoKG that augments graph embeddings [Iliakis, 2022] and cross-disciplinary data integration within the OKN framework (Section 5.3).

This paper aims to provide guidelines and examples for implementing and utilizing S2 in GeoKGs, highlighting its analytical advantages. By doing so, it seeks to advance GeoAI and offer a scalable solution for managing and analyzing large-scale geospatial data within GeoKGs.

The rest of the paper is structured as follows: Section 2 provides background on GeoKGs and DGGS frameworks, highlighting KWG and S2 Geometry. Section 3 introduces the workflow for modeling and ingesting S2 data into KWG, along with the technical strategy for quantization. Section 4 discusses the implementation of the two quantization methods in KWG. Section 5 evaluates the performance and benefits of S2 integration through various use cases, demonstrating improvements in data processing, query efficiency, and scalability. Finally, Section 6 discusses the broader implications of using DGGS, particularly S2 Geometry, within GeoKGs, including achieved benefits, current limitations, and areas for future research.

2 Theoretical Background and Related Research

2.1 Geospatial Knowledge Graphs

Geospatial knowledge graphs (GeoKGs) emerged in the late 2000s as open data ecosystems, primarily aiming to democratize data access in alignment with FAIR (Findable, Accessible, Interoperable, Reusable) data principles [Wilkinson et al., 2016]. Early graphs such as GeoNames⁷ and LinkedGeoData⁸ predominantly comprised *explicit geographic* entities, such as named places, natural features, landmarks, roads, and historical features, with point geometries and limited semantics. In recent years, GeoKGs have expanded in scope to model *geographically themed* data across many domains, such as from environmental [Janowicz et al., 2022, Zhu et al., 2021a], public health [Jiang et al., 2020, Zhu et al., 2022a], disaster management [Janowicz et al., 2022], transportation [Böckling et al., 2024, Qi et al., 2023], production logistics [Zhao et al., 2022], and gaming domains [Jiang et al., 2020] demonstrating the versatility and impact of GeoKGs in various application areas. These GeoKGs play a pivotal role in cross-domain geospatial analytics [Janowicz et al., 2022], geospatial question answering [Mai et al., 2021, Weinberger et al., 2022], and geo-visualization [Balla et al., 2020, Li et al., 2023]. Moreover, their rich contextual information makes them essential training data for spatial models, facilitating the development of spatial and temporal reasoning [Zhu et al., 2022b], predictive analytics, and decision support systems [Zhu et al., 2022b, Mai et al., 2022]. Examples of such rich GeoKGs in the OKN ecosystem [U.S. National Science Foundation, November 2018] include the KWG⁹ that focuses on environmental intelligence [Janowicz et al., 2022]; the UF-OKN¹⁰ for flood prediction, response, mitigation, and prevention [Saksena, 2022]; and the Safe Agricultural Products and Water Graph¹¹ (SAWGraph) to understand per- and polyfluoroalkyl substances (PFAS) contamination in food and water systems.

A. Preliminaries of the RDF Data Model: The structure and principles of RDF and the Web Ontology Language (OWL) [Hitzler et al., 2009] directly influence how S2 is used to synthesize, integrate, and query data within KWG, as will be discussed later in Section 4. To facilitate understanding, this section briefly introduces the basic components and structure of RDF and SPARQL. For a more comprehensive introduction to RDF and SPARQL, refer to [Manola et al., 2004, Hitzler et al., 2010, World Wide Web Consortium and others, 2013].

Definition 2.1. *RDF triple:* An RDF triple $t(s, p, o)$ is the basic atomic entity of a knowledge graph. It expresses a single statement about semantic data. The subject (s) and object (o) are considered graph vertices referring to a resource or a simple value (called literal), and the property (p) (a.k.a. predicate) is the directed edge that connects the two vertices. The *resources* in $t(s, p, o)$ are given uniform resource identifiers (URI) or are blank nodes (denoting an unknown resource).

Definition 2.2. *RDF graph:* An RDF graph is a collection of RDF triples. Such a graph can essentially be viewed as a directed graph $G = (V, E)$ where V denotes the set of vertices that can be resources or literals, and E denotes the set of directed edges.

Definition 2.3. *SPARQL query:* A SPARQL query Q is defined as tuple $Q = (E, G, R)$. E denotes the algebraic expression built from graph patterns and solution modifiers. G is the RDF graph being queried. R denotes the result form, such as SELECT, CONSTRUCT, DESCRIBE, or ASK, which specifies how the query results are processed and

⁷<https://www.geonames.org/>

⁸<http://linkedgeodata.org/>

⁹<https://knowwheragraph.org/>

¹⁰<https://ufokn.com/>

¹¹<https://sawgraph.github.io/>

presented. The algebraic expression E can include various graph patterns and solution modifiers like PROJECTION, DISTINCT, LIMIT, or ORDER BY. The simplest graph pattern in SPARQL is the triple pattern, which matches triples in the RDF graph.

B. GeoSPARQL: In the RDF domain, OGC’s GeoSPARQL standard [Car and Homburg, 2022] is the leading specification for representing and querying geospatial data. It is implemented as an extension by many RDF graph databases [Jovanovik et al., 2021]. GeoSPARQL leverages OGC’s Simple Features ontology¹² for defining spatial entities as shown in Figure. 1. The `geo:SpatialObject` class includes any resource that can have a spatial representation. The `geo:Feature` class specifically represents spatial objects with concrete geographical shapes, linked to their geometries (serialized as GML or WKT) via the `geo:hasGeometry` property. GeoSPARQL supports qualitative relations such as containment and overlap for evaluating topological relationships between entities, with `geo:spatialRelation` subsuming specific properties. Additionally, the specification provides properties for non-topological spatial operations (e.g., distance, buffer) and spatial aggregation functions. GeoSPARQL can be used in conjunction with OWL to develop detailed ontologies that enhance and constrain spatial data.

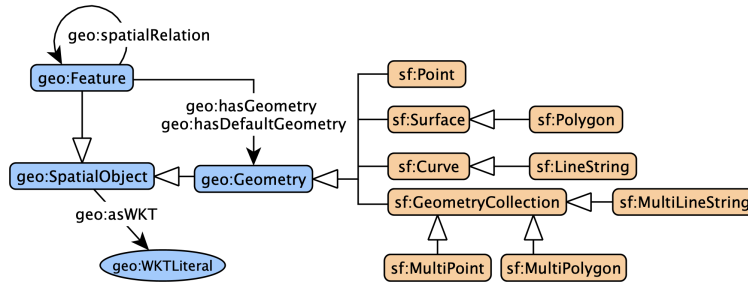


Figure 1: GeoSPARQL’s core concepts are shown in blue boxes, and Simple Features geometry classes in beige boxes. White-headed arrows represent `rdfs:subClass` relations, while filled arrows denote object or data properties

C. Spatial Query Challenges in GeoKGs: The size of GeoKGs can increase significantly when handling complex geometries, such as multi-polygons and polylines. For instance, the geometric representation of Greece from GADM¹³ is a multi-polygon consisting of 695 individual polygons, with approximately 29,900 vertices. This results in a Well-Known Text (WKT) representation that is about 9MB in size. High precision can adversely affect the graph’s performance in terms of storage, indexing, and query efficiency [Regalia et al., 2017], while reducing precision can impact the quality of spatial querying. Algorithms determining topological relations using geometries operate with polynomial time complexity relative to the number of nodes in the geometries being tested [Rigaux et al., 2002]. Graph databases that implement popular space-dividing indexing mechanisms, such as quadtrees and geohashing (e.g., GraphDB), still encounter limitations in spatially pruning search spaces. Geohashing can split regions of interest across multiple cells, leading to boundary issues where a single spatial entity is divided by cell boundaries. This affects the accuracy and efficiency of spatial queries, as additional computation is needed to merge or handle entities spanning multiple geohashes [Papadias et al., 2003]. This is particularly problematic for linear features (e.g., rivers) or extensive areas (e.g., country boundaries). Each geohash string is independent, lacking a hierarchical relationship between different levels of resolution, and they are not ordered based on spatial proximity. This non-intuitive ordering complicates range queries and neighborhood searches, especially for features such as political borders that often span multiple geohash cells [Acharya, 2023]. Quadtrees provide adaptive resolution indexing capabilities and improve query performance by reducing the number of nodes that need to be inspected. However, high-resolution data can result in very deep quadtree structures, which can lead to performance bottlenecks, particularly in large-scale graphs [Dinkins, 2023]. Experimental evaluations have also shown that spatial joins for complex geometries are not optimized in GeoSPARQL-compliant RDF databases [Huang et al., 2019, Ioannidis et al., 2021, Li et al., 2022a]. These size-related query challenges of GeoKGs re-emphasize prior statements [Regalia et al., 2019] that storing accurate representations of geospatial data in their original vector or raster format, including complex geometries as RDF literals, while reasonable, may not be suitable for storage and query efficiency.

¹²<https://www.ogc.org/standard/sfa/>

¹³<https://gadm.org/data.html>

2.2 The KnowWhereGraph

Envisioned as a *gazetteer of gazetteers* that links heterogeneous data via joint place identifiers, KnowWhereGraph (KWG) empowers decision-makers with on-demand and comprehensive location insights derived from a diverse range of data. By minimizing data processing overhead, KWG provides semantically rich, contextualized, and analysis-ready data for environmental intelligence analytics, with a particular focus on two key use cases. The humanitarian relief use case [Zhu et al., 2021b] is tailored to aid humanitarian organizations in swiftly identifying and mobilizing relevant personnel with suitable expertise to respond effectively to imminent or ongoing disasters. The farm-to-table use case [Janowicz et al., 2022] aims to address concerns regarding the safety of crops affected by smoke and ash from wildfires, providing crucial insights for stakeholders along the supply chain. The graph is implemented in GraphDB, an RDF graph database that supports SPARQL 1.1 and GeoSPARQL. The SPARQL endpoint to the graph is <https://stko-kwg.geog.ucsb.edu/graphdb/sparql>.

KWG includes data about a wide range of *region identifiers*, encompassing global administrative regions, climate divisions, weather forecast zones, census statistical areas, federal judicial districts, and zip code areas. Other feature data include hazard events, road segments, and public health departments. The graph also integrates a set of geographically themed data that significantly influences the use cases. These encompass observation and measurement data, such as climate observations, air quality indices, public health metrics, and natural hazard impacts. Figure 2 is an abstracted pattern of the KWG Ontology [Shimizu et al., 2023] depicting how: 1) entities with explicit geometries are modeled using GeoSPARQL, and 2) environmental observations are modeled using the SSN/SOSA ontology [Janowicz et al., 2019, Haller et al., 2019]. At the heart of this pattern is the core class `kwg-ont:Region`, which encapsulates dataset-specific subclasses of regions. Qualitative spatial relations or simply topological relations between features are established using the set of DE-9IM relations denoted as $\mathcal{T} = \{\text{kwg-ont:sfWithin}, \text{kwg-ont:sfContains}, \text{kwg-ont:sfTouches}, \text{kwg-ont:sfCrosses}, \text{kwg-ont:sfOverlaps}, \text{kwg-ont:sfIntersects}\}$. Relations in \mathcal{T} are sub-properties of the generic `kwg-ont:spatialRelation` within the `kwg-ont` namespace. Each relation follows the naming convention of its topological counterparts in GeoSPARQL, e.g., `kwg-ont:sfContains` is semantically analogous to `geo:sfContains`. However, the spatial relations in the `kwg-ont` namespace are decoupled from GeoSPARQL’s relations (i.e., they are not axiomatically related) to prevent interference with inferencing in the latter’s inbuilt functions. Much of the observation data in KWG are not feature-based but have spatial information encoded through identifiers such as ZIP code, FIPS code, and geoid. These identifiers allow thematic data to be linked to their associated region identifiers. Observation data are georeferenced to their corresponding geographical feature of interest using SOSA’s `sosa:hasFeatureOfInterest` property as shown in Figure 2. This observation-centric linking paradigm is uniformly applied across all data with a spatial dimension [Janowicz, 2012].

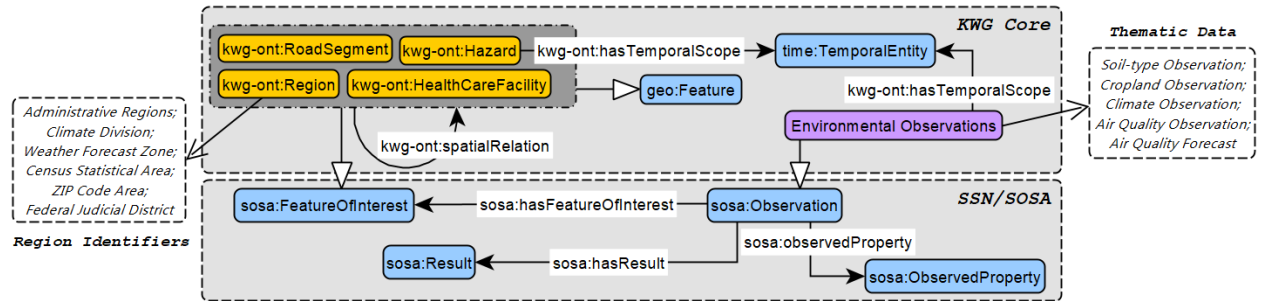


Figure 2: Schema diagram that denotes the core concepts/themes in KWG (explicit geographic features denoted using yellow boxes and geographically themed observations denoted using the purple box) and their extension of SSN/SOSA, GeoSPARQL, and OWL-Time ontologies (denotes using blue boxes). The SSN/SOSA pattern denotes the generic graph to query KWG observations. White-headed arrows denote `rdfs:subClass` relationships.

Regions are spatially cross-integrated, allowing thematic data to also be cross-linked. For instance, census statistics or climate observations can be analyzed together, but this can be conflicting since different types of regions are of different scales but also discretized for distinct purposes (e.g., weather forecast zones are delineated based on differences in weather, while census statistical areas are delineated based on the number of inhabitants and urbanization). By using the S2 Geometry all the disconnected themes and layers are harmonized onto a common discretized spatial unit of analysis that is unbiased by natural and human processes. This quantization of KWG data onto S2 cells will be discussed later in Section 4.

Total number of triples in the graph	28,643,164,592
Number of regions (i.e., instances of <code>kwg-ont:Region</code>) in the ABox	438,927
Number of features (i.e., instances of <code>geo:Feature</code>) in the ABox	48,397,918
Number of features of interest (<code>sosa:FeatureOfInterest</code>) in the ABox	6,705,844
Number of geometries (i.e., instances of <code>geo:Geometry</code>) in the ABox	48,077,280
Number of point geometries (i.e., instances of <code>sf:Point</code>) in the ABox	8,424,208
Number of lines (i.e., instances of <code>sf:LineString</code>) in the ABox	741,214
Number of simple polygon geometries (i.e., instances of <code>sf:Polygon</code>) in the ABox	38,546
Number of complex polygon geometries (i.e., instances of <code>sf:MultiPolygon</code>) in the ABox	37056438
Number of observations (i.e., instances of <code>sosa:Observation</code>) in the ABox	254,006,244

Table 1: KnowWhereGraph (v 3.0 or KWG - Santa Barbara) statistics (from 09/15/2023).

Table 1 provides an overview of KWG graph statistics (in terms of the number of total triples, feature nodes, geometry nodes, and observation nodes). The number of complex geometries (polylines/multi-polygons) is an indication of the size and complexity of the graph.

2.3 Discrete Global Grid Systems

A Discrete Global Grid (DGG) is a spatial reference system that tessellates the Earth’s surface into a series of discrete, connected, and well-aligned cells. A DGGs is a hierarchical composition of multi-resolution DGGs. At the core of a DGGs are the concepts of cells, levels, and coverings. A *cell* is a fundamental unit in a DGG and represents a specific geographic region with a fixed location and area. Each DGG layer corresponds to a *level* representing the granularity of cells in that layer. Cell sizes and cell counts vary between levels. Each cell at a parent level is linked to a cell at the next level with a finer predefined resolution, allowing for efficient hierarchical operations. Cells are uniquely identified by stable cell identifiers (cell IDs) that provide information regarding the hierarchical level, and structural connections to parents and neighboring cells. The collection of cells that covers a given region or shape is a *covering*. A DGGs is *congruent* if and only if each cell at resolution k consists of a union of cells at resolution $k + 1$. A DGGs is *aligned* if and only if each point within a cell at resolution k is also with its child cell at resolution $k + 1$ [Sahr et al., 2003]. The congruence and alignment properties of cells differ between various DGGs (see a comparison presented in Figure 3).

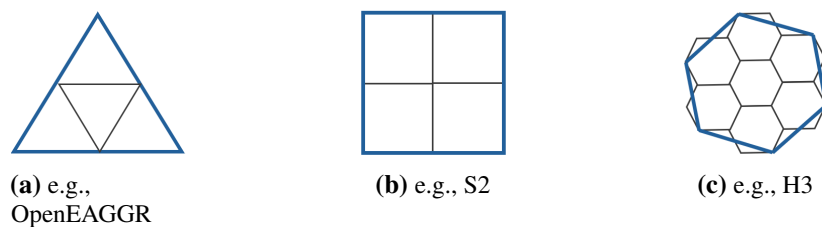


Figure 3: Congruence (i.e., parent-child containment relationships), and aggregation or decomposition resolutions (e.g., squares can be aggregated in groups of four to form coarser resolution objects) in DGGs with varying polyhedron shapes.

The design of a DGGs is primarily governed by the base polyhedron (cube, dodecahedron, icosahedron, octahedron, and tetrahedron) adopted for the spherical approximation of the Earth, and the method adopted to partition the polyhedron into finer cells. The latter choice determines the cell type (square, triangle, or hexagon), aggregation or decomposition resolutions, and congruence properties as compared in Figure 3. Other design choices such as methods of orienting the polyhedron relative to the surface of the Earth, and methods to transform the partitioned planar cells to the sphere are equally important as they determine the level of area, shape, and angular distortion that can impact downstream spatial analysis. DGGs primarily use hierarchy-based, coordinate-based, or space-filling curve-based indexing systems [Mahdavi Amiri et al., 2019]. DGGs frameworks that use a space-filling curve, for instance Hilbert curve (adopted in S2), and Gosper curve (adopted in H3), provide an explicit structural ordering of cells along the path of the curve. A

cell’s position (or coordinates) along this curve uniquely determines its cell ID, and resolution. Space-filling curves map n -dimensional spatial data to a one-dimensional sequence of cell IDs, approximately preserving the spatial locality of the data points [Uher et al., 2019]. This transformation provides an efficient method for indexing and querying geographic information. Different DGGs offer different performance capabilities for different objectives, e.g., rHEALPix for latitudinal data analysis [Bowater and Stefanakis, 2019] and area-based statistics [Gibb, 2016], H3 for modeling of movements through the grid [Kmoch et al., 2022], and S2 for smoother multi-resolution analysis [Kmoch et al., 2022].

The OGC’s DGGs standard [OGC, 2017] specifies three core operational requirements for DGGs specifications: quantization, spatial relation, and interoperability operations. *Quantization operations* assign raw or synthesized vector and raster spatial data to DGGs cells. *Spatial relation operations* utilize the hierarchical and connected structure of cells and cell typologies to facilitate cell traversal and spatial analysis functions. Interoperability operations are designed to communicate with end-users or other spatial data infrastructures via standard APIs and data formats. Most DGGs have open-source software libraries as well as bindings in various programming languages that provide methods for these operations. For example, the H3 library¹⁴ is implemented in C and the S2 library¹⁵ in C++. Existing works have reviewed the operations supported by the state-of-the-art DGGs libraries, their adherence to the OGC standard [Li and Stefanakis, 2020], and trade-offs of their different characteristics designs [Bondaruk et al., 2020, Kmoch et al., 2022].

DGGs in Traditional Geospatial Applications: In the last two decades, DGGs have been instrumental in actualizing the Digital Earth vision [Goodchild, 2000] through their implementations in sensor data integration [Kraft et al., 2019]; multi-dimensional vector big data management [Robertson et al., 2020, Sirdeshmukh et al., 2019]; storing pre-aggregated results [Kraft et al., 2019, Robertson et al., 2020]; advanced multi-resolution geo-visualization [Raposo, 2019, Li et al., 2022b]; incorporating spatial uncertainty in big data analysis [Robertson et al., 2020]; and storing, fusing, and rendering raster data [Strassburg et al., 2010, Li et al., 2021, Rawson et al., 2022, Bousquin, 2021, Miao et al., 2023]. Specific application domains implementing DGGs include terrain data modeling [Li et al., 2021, Lin et al., 2018], ecological studies [Kranstauber et al., 2015, Birch et al., 2007], environmental observations modeling [Lin et al., 2018, Romanov and Khvostov, 2018], ride-hailing services [Pereira et al., 2024], and geo-social networking [Woźniak and Szymański, 2021].

DGGs in GeoKGs: More recently DGGs have been adopted in GeoKGs for many disciplines and applications. The ISEA3H DGGs is adopted to provide a standardized representation of national multi-source terrain data in [Li et al., 2021]. Elevation data from multiple raster datasets are quantized on the grid by resampling with bilinear interpolation at the cell centroid locations. [Han et al., 2022] uses the GeoSOT-3D DGGs to integrate spatiotemporal information in the airspace environment for selecting airport sites in response to emergencies. The Spatial-Temporal Knowledge Graph (STKG) in [Böckling et al., 2024] adopts KWG’s methodology to transform Open Street Map (OSM) data onto the H3 grid by topologically linking OSM geometries to grid cells via spatial predicates defined by GeoSPARQL. However, the relations between the grid cells use a set of non-topological relations. Due to the non-congruency of H3 cells, inferring spatial relations across multiple resolutions is not straightforward. This necessitates precomputing the links between OSM geometries and grid cells at several levels, resulting in a very large graph. AugGKG is another example that integrates spatio-temporal data on the GeoSOT for spatio-temporal question answering by creating sub-knowledge graphs on each time slice [Han et al., 2023]. Wāhi, a discrete global grid gazetteer [Adams, 2017] links places in the GeoNames database to each level of three DGGs (ISEA3H, ISEA4H, ISEA4T). Links were created using two types of spatial footprints of places in the gazetteer. The first type is defined by the grid cells that spatially intersect with the source geometry, which can be polygons (when available) or points, and will always cover the source polygon. The second type is defined by the spatial intersection of the centroids of grid cells with geographic features represented by polygons. If no centroid intersects, the single cell with the closest centroid is matched to the feature. This second type of footprint is always smaller or equal in size to the first type and is not guaranteed to cover the entire source polygon. Due to the current unavailability of the server hosting Wāhi, we were unable to determine the exact predicate used to bin point data into cells. The data is stored in a PostgreSQL PostGIS database, with the option to export data into GeoJSON-LD format.

2.4 The S2 Discrete Global Grid

Google’s S2 Geometry defines a sophisticated system for tessellating the Earth into a hierarchical mosaic of S2 cells, which are specialized spherical quadrilaterals (Figure 4a). The edges of these cells are geodesics, meaning they follow the shortest path along the sphere’s surface. This hierarchical mosaic is constructed through a nested structure, where each cell acts as a node within a quadtree, and each non-child node can be recursively subdivided to form four child cells. S2 cells are sequentially indexed on a Hilbert space-filling curve that traverses the unit sphere’s surface projected

¹⁴<https://h3geo.org/>

¹⁵<https://s2geometry.io/>

onto the six faces of the cube using the Quadrilateralized Spherical Cube (QSC) projection method. This projection ensures a relatively even distribution of cells across the sphere’s surface, maintaining geometric consistency and balance. Each S2 cell is uniquely identified by a 64-bit S2CellID, which encodes the cell’s location on the curve and its level within the S2 hierarchy. The average area of cells within each level ranges from approximately $8.5 \times 10^7 km^2$ at level 0 to about $0.74 cm^2$ at level 30.

For quantization operations and semantic compression in GeoKGs, S2 Geometry offers significant advantages [Zalewski et al., 2021]. Distance and area calculations in WGS84, the most commonly used coordinate reference system (CRS) in GIS, require geodesic computations on an ellipsoid, which can be computationally expensive for large datasets. In contrast, S2 Geometry simplifies these calculations by approximating distances and areas on a unit sphere. Although this results in slightly less accurate measurements, it significantly improves computational efficiency. The regular hierarchical structure of S2 ensures that point-in-cell relationships are preserved across multiple resolutions, enabling reliable and scalable qualitative spatial querying. Additionally, the near-equal area of S2 cells is critical for statistical aggregations, such as approximating quantities within a cell by summing over all child cells.



Figure 4: **(a)** Hierarchical tessellation of the Earth using the S2 Geometry. **(b)** The S2Cell hierarchy projecting the Earth onto six “base cells”. These illustrations are adopted from the S2 Library documentation [Veach et al., 2017].

The core S2 Geometry library, licensed under the open-source Apache License 2.0, is written in C++ [Veach et al., 2017]. Wrappers for this library are available in Python, Java, JavaScript, R, and other languages at varying levels of maturity. The primary purpose of the S2 library is to provide operations for computational geometry and spatial indexing on the sphere. The S2 library supports the following geospatial functionalities:

- Representations of angles, intervals, and geometric shapes (e.g., points, polylines, polygons) both on the unit sphere and in latitude–longitude space.
- Constructive operations (e.g., union, difference, buffer), boolean predicates for testing topology relationships (e.g., containment, intersection), and mathematical predicates for evaluating spatial relationships (e.g., distance within a threshold, point-in-region) for arbitrary geometric objects.
- Algorithms for measuring areas, calculating distances, computing centroids, simplifying geometry, and finding nearby objects.
- Functions for cell navigation (retrieving parent, children, and neighboring cells), and traversing cells at the same level along the Hilbert curve.
- Support for spatial indexing, including conversion between geographic coordinates and S2 cells, and the ability to approximate arbitrary regions as unions of S2 cells (see Figure 4b).

3 Methodology

This section outlines the technical aspects of integrating and utilizing S2 within KWG. It provides an overview of how S2 geometry is modeled and ingested into KWG, followed by a discussion of the general technical approach for implementing various quantization methods. These methods will be further detailed in Section 4.

3.1 Conceptual Schema for the S2 Geometry in KnowWhereGraph

GeoSPARQL 1.1 [Car and Homburg, 2022] introduces the `geo:asDGGs` property to link a DGGs cell to its cell ID serialization in the `geo:dggLiteral` datatype. However, GeoSPARQL does not natively interpret DGGs literals, necessitating external implementations for handling them. Currently, GeoSPARQL-DGGs [David Habgood] is the only library available that leverages RDFlib to support GeoSPARQL’s topological functions on DGGs literals, but it is limited to the rHEALPix DGGs. Given this limitation, we chose to represent S2 cells as vector geometries (with cell vertices forming a polygon) using the WKT specification. This approach ensures compatibility with existing geospatial standards and tools, providing a robust solution for integrating S2 cells within GeoSPARQL-extending frameworks such as KWG.

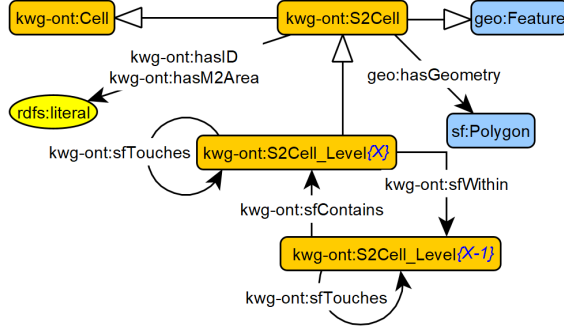


Figure 5: Schema diagram illustrating the extension of GeoSPARQL concepts to model S2 data.

The schema diagram in Figure 5 represents the conceptual modeling of the S2 Geometry in KWG. The primary class, `kwg-ont:S2Cell`, is defined as a subclass of `geo:Feature` and `kwg-ont:Cell`, generalizing cells in a DGG [Shimizu et al., 2021]. The geometry of each S2 cell is a simple feature polygon. The more detailed geometric representation of S2 cells is adopted in KWG primarily for visualization needs, but if visualization and runtime topological querying are not a priority this geometry can be abstracted to a point. `kwg-ont:S2Cell` is further specialized into subclasses denoted as `kwg-ont:S2Cell_Level{X}`, where X indicates various levels in the S2 hierarchy. Cells are structurally connected both within and between levels via DE-9IM relationships from the KWG ontology (Figure 2). Hierarchical *parent-child* relationships between S2 cells are represented by `kwg-ont:sfContains` and `kwg-ont:sfWithin`, while *neighbor* relationships are expressed using `kwg-ont:sfTouches`. Hierarchical connectivity is explicitly precomputed up to one level, while multi-level connectivity is inferred via the transitive properties defined on `kwg-ont:sfContains` and `kwg-ont:sfWithin`. In a reasoning-enabled GraphDB repository, these inferred relationships are pre-materialized through forward-chaining during the data loading process. Additionally, each S2 cell is annotated with its identifier and area using the data properties `kwg-ont:hasID` and `kwg-ont:hasM2Area`, while the cell resolution is implicit in the class name.

The `s2sphere`¹⁶ python implementation of the S2 Geometry library is used in generating the S2-RDF graph, a subgraph in KWG. Figure 6 illustrates one S2 cell from the graph displayed on a map via KWG’s dereferencing application. The snapshot also displays the attributes and linkages between the cell and other features in the graph.

3.2 Challenges

Using S2 cells as polygon geometry representations in WKT serialization introduces certain ambiguities. The discrepancies between edges in planar and spherical spaces can result in indexing challenges and visualization artifacts, which are discussed in this section.

Indexing: The default CRS for WKT literals is WGS84. Geographic coordinates in WGS84 span from 180° to 180° longitude and -90° to 90° degrees latitude, but some S2 cells span the antimeridian ($\pm 180^\circ$) and the poles. Since indexing in GraphDB uses WGS84, indexing issues with cells that cross the antimeridian or the poles because they are not normalized (either through wrapping or splitting) rendering them topologically invalid. Figure 7a illustrates an example of an S2 cell crossing the antimeridian that cannot be indexed in the graph. This issue occurs when the longitude difference between two consecutive points in the path is $\geq 180^\circ$. In spatial databases like GraphDB, this

¹⁶<http://s2sphere.readthedocs.io/>

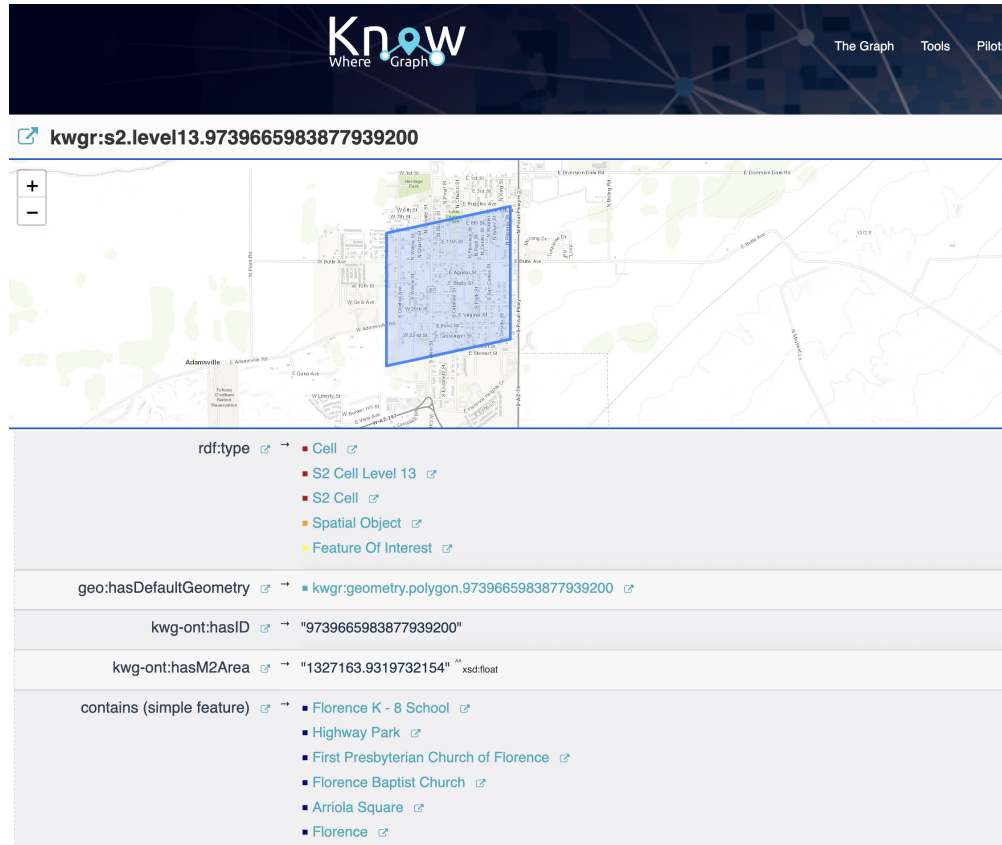


Figure 6: S2 cell with cell ID 9739665983877939200 visualized within KWG’s phuzzy dereferencing application.

ambiguity must be resolved to ensure accurate representation and querying. Possible solutions include splitting S2 cells at the antimeridian or representing them as points.

Visualization Artifacts: When S2 cells are visualized on maps with a Mercator projection, as in most web maps, their true shape and size on the sphere may not be accurately reflected, with more pronounced distortion at higher latitudes. S2 uses geodesic edges, meaning that the edges of the cells follow the shortest path on the spherical Earth approximation. On a Mercator projection, geodesic paths in the east–west direction, except at the Equator, appear as curves bulging towards the poles. Consequently, the “horizontal” edges of S2 cells appear curved towards the poles (Figure 8b). When S2 cells are represented by straight lines connecting their four corner vertices in a Mercator projection, their east–west edges are incorrectly rendered as rhumb lines, or paths that follow a constant bearing relative to north, like lines of latitude (Figure 8a). This shape distortion can lead to potential misinterpretations of the spatial data. For example, points that are topologically within an S2 cell may appear to lie outside the cell, and vice versa (an example using the state of Illinois is compared in Figure 8). Additionally, S2 quadrilaterals do not tessellate perfectly on planar maps, leading to gaps or overlaps between cells. Figure 7b denotes another visualization artifact, where an S2 cell that crosses the antimeridian appears stretched across the world when represented on a flat map that uses Mercator map projection.

3.3 Technical Strategy for Data Quantization in KnowWhereGraph

S2 in KWG facilitates efficient data storage and retrieval through different data quantization strategies. As previously mentioned, indexing and query operations provided by the S2 Geometry are not natively available within GraphDB. Quantization is adapted in the KWG environment by way of view materialization [Ibragimov et al., 2016], where triples — spatial, temporal, thematic, or their combinations — are pre-computed using the `s2sphere` library and persisted within the graph. These materialized views enhance the scalability of query processing, particularly for complex spatial analytic operations, by circumventing direct access to geometric data (e.g., WKT literals) within the graph. We employ

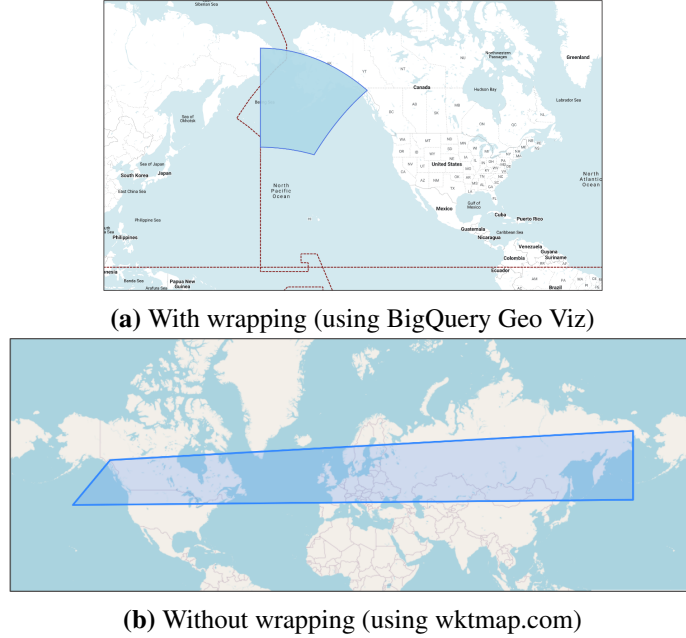


Figure 7: S2 cell with cell ID 9007199254740992000. Its WKT serialization is `'POLYGON((180 67.3801, 180 45, -157.3801 42.7093, -135 59.4910, 180 67.3801))'` `geo:wktLiteral`.

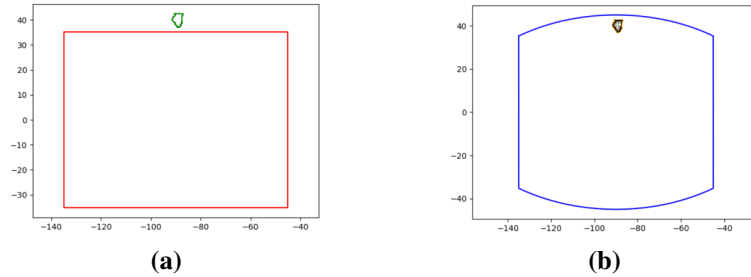


Figure 8: Visualization artifacts when geodesic edges of S2 cells are considered as rhumb lines, or paths of constant bearing relative to north. (a) Illinois is not inside S2 cell, level 0, hex 9, which has straight-edge boundaries. (b) Illinois is within S2 cell, level 0, with cell ID hex 9, showing geodesic boundaries. Hex refers to the hexadecimal representation of the S2 cell ID.

tailored ontology patterns [Falbo et al., 2013] to guide the selection of views for materialization [Lan et al., 2022]. These patterns, detailed in Section 4, delineate different ways for quantizing data to S2 cells. Nodes in a pattern depict frequently accessed relationships (based on use-case needs) or spatial joins earmarked for materialization, thereby mitigating query latency.

Precomputation of triples also facilitates data conflation by consolidating vector, raster, and other geographically themed datasets at the intersection of the S2 grid. This process enriches the graph, improving the efficacy of graph-based algorithms such as similarity detection and clustering, and fostering serendipitous discoveries across interconnected data entities. Unlike the space costs associated with relational databases, materializing views in a graph database also allows for data compression, which would be impossible if data were ingested with their original structure and precision. Whether for enrichment or compression, the choice of pattern depends on a nuanced consideration of factors such as on-the-fly computation overheads, graph size, and graph maintenance.

4 Implementing Data Quantization on S2 in KnowWhereGraph

In this section, we elaborate on the two quantization strategies adopted in KWG, the ontology patterns adopted for materializing views, and their specific benefits.

4.1 Topological Enrichment of Vector Data

Research on computational time and space trade-offs in GeoKGs has demonstrated that precomputation of topological relations can yield significant performance benefits [Regalia et al., 2016, 2019]. Traditionally, places (represented as `kwg-ont:Region` nodes in KWG) have been central for topologically linking other spatial features (e.g., `kwg-ont:Hazard` and `kwg-ont:RoadSegment`) within GeoKGs [Regalia et al., 2019]. However, place boundaries are inherently dynamic, meaning their topological relationships with intersecting features can change over time. For instance, before 2011, South Sudan was spatially *within* Sudan, but after gaining independence, the relationship changed to a border-sharing or *touches* relationship. In contrast, S2 cell boundaries are fixed and immutable, providing a stable spatial framework for linking features and supporting multi-resolution and hierarchical spatial reasoning [Timpf and Frank, 1997].

The S2 grid at level 13 is selected as the reference layer, offering an appropriate level of detail ($\sim 1.27 \text{ km}^2$ per cell) for topologically interlinking KWG data. From this point forward, cells in this layer will be referred to as S2 reference cells. *Topological enrichment of vector data* is achieved by precomputing and materializing topological relations between entities with explicit geometries and S2 reference cells in the graph, creating a dense network of interconnected spatial objects. The spatial relations utilized are a subset of topological relations from \mathcal{T} (see Section 2.2), which are sub-properties of `kwg-ont:spatialRelation`. Figure 9a illustrates the ontology pattern for this view materialization. Certain datasets ingested into KWG (e.g., public health departments, and pharmacies) provide addresses or other location-based information, such as ZIP codes, which are geocoded into point coordinates for topological linking to S2 cells.

Figure 9b represents the OWL properties [Hitzler et al., 2009] defined over the topological relations in \mathcal{T} . We precompute most of the implicit triples induced by properties to reduce graph initialization costs (*total materialization* at load time). We leave the triples resulting from the transitive property (on `kwg-ont:sfWithin`) to be entailed from forward chaining during graph initialization.

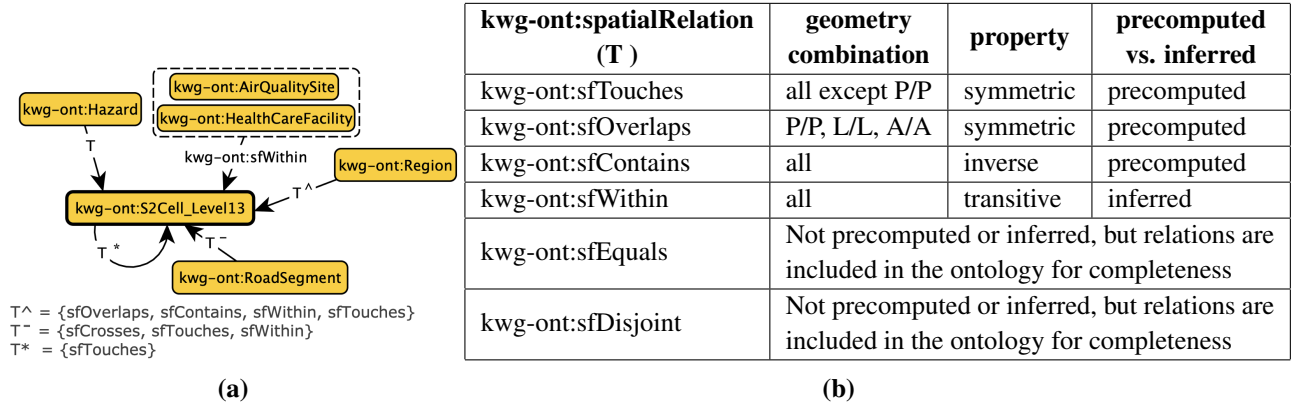


Figure 9: (a) Ontology pattern for topologically enriching vector geographic entities. (b) Table showing the properties asserted on topological relations in KWG for various geometry type combinations (P-Point, L-Curve, A-Surface) and the corresponding A-Box triples that are materialized.

This enrichment, although it may significantly increase the number of triples in the graph, makes feature geometries obsolete, thereby enhancing querying and data processing speed. Table 2 shows the spatial query speedups achieved through topological enrichment.

Query type	Query details	No. results retrieved (via S2)	Query time (via S2)	No. results retrieved (via GeoSPARQL)	Query time (via GeoSPARQL)
P/A	hospitals in Santa Barbara [Q1]	22	0.3 secs	23	30 secs
L/A	roads intersecting Santa Barbara [Q2]	1747	5.7 secs	-	Timeout
A/A	statistical areas overlapping Santa Barbara [Q3]	4	1.9 secs	4	5.8 secs

Table 2: Querying the graph using S2 (with topological enrichment) versus using spatial functions from GeoSPARQL. Queries are available in the following Github repository:

<https://github.com/shirlysteph/s2-kwg/tree/main/demos/sample-queries>

A. Optimized Topological Enrichment:

Classic topological enrichment uses S2 cells at level 13, but applying this resolution to large polygons, such as drought or smoke plume areas, can result in inefficiencies due to the massive data volumes involved. For example, a temporally sliced multi-polygon representing drought could cover up to 6.8 million square kilometers of the contiguous United States. To improve efficiency, a discrete and compressed enrichment framework [Zalewski et al., 2021] is employed, combining DE-9IM with hierarchical S2 cell nesting. This method links large polygons to the largest S2 cells at coarser resolutions, leveraging the transitivity of within/containment relations in the spatial ontology to infer triples describing spatial relationships between the region and S2 reference cells. This approach reduces data volume and speeds up computations by limiting the number of cells processed in each query.

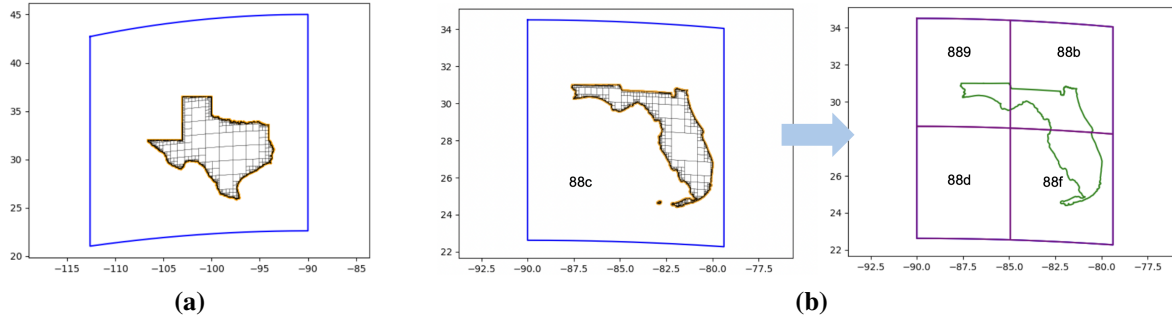


Figure 10: Examples of optimized topological enrichment: (a) Texas is covered with S2 cells at various levels for efficient representation. (b) Florida is similarly covered with S2 cells at different levels and is contained within one S2 cell at level 3 (hex 88c), while overlapping four S2 cells at level 4 (hex 889, 88b, 88d, 88f).

B. Computational Method for Boolean Topological Relationships: The S2 Geometry library provides classes for representing shapes (points, curves, and regions) on the Earth’s surface. These shapes are defined using points and geodesic curves, which presents challenges when working with vector data serialized in the WGS84 format, as these data do not inherently conform to geodesic boundaries. To address this incompatibility, we developed a custom algorithm to compute topological relationships (based on the DE-9IM) between the S2 reference cells and geometric objects in KWG. This algorithm leverages the `s2sphere` python wrapper for the library alongside `Shapely`, which handles planar geometric objects. Key methods from the S2 library’s `S2RegionCoverer` class, such as `GetCovering` and `GetInteriorCovering`, were instrumental in generating `S2CellUnion` objects that either cover or are contained within the specified region. The technical steps of the algorithm are as follows:

1. **Geometry approximation:** Each WGS84 geometry ([multi-]point, [multi-]line, [multi-]polygon) is approximated as its analogous S2 object(s) on the unit sphere. In the case of polygons, the boundary is segmented by adding vertices such that the distance between any two consecutive vertices does not exceed a specified tolerance. This ensures that linear edges are replaced by geodesic curves that closely approximate the original planar shapes.
2. **Creating coverings:** The `S2RegionCoverer` is then used to approximate the S2 object as unions of S2 reference cells, known as cell coverings. This includes ordinary coverings (cells at various levels that cover the geometry), homogeneous coverings (cells that cover the geometry at a specified level), and interior coverings (cells at various levels strictly within the geometry).
3. **Topological relationship computation:** For point data, each point is directly mapped to an `S2Point` and associated with an `S2CellID` at the maximum resolution level. For line and polygon data, topological relationships are computed by identifying overlapping or contained cells using the coverings generated. For example, to identify the cells at a specified level that are strictly within the given shape, an interior covering is used. Overlaps are determined by the difference between homogeneous and interior coverings.

4.2 Grid-Based Data Discretization

Data discretization involves transforming non-DGGS spatial data (vector or raster) through different transformation strategies (statistical aggregation, decomposition, spatial overlay, etc.) to represent them as S2 cell-based gridded data for flexible representation and analysis while maintaining spatial relationships and scalability across different resolutions. Cells are indicated as the `sosa:FeatureOfInterest` [Janowicz et al., 2019] to which various data values are mapped, via object properties or data properties. These data values can be 1:1 grid mapping (for raster cells),

aggregated summaries, or multi-level decomposition — see examples in Figure 11. Quantized values can be quantitative (e.g., area covered by a smoke plume) or qualitative details (e.g., categorical data related to soil porosity).

Vector data in KWG spans a wide range of scales, from large-scale features like smoke plumes covering extensive areas to highly localized data such as wildfire events represented as points or small polygons. Although wildfires are a primary source of smoke plumes, their spatial and temporal distributions provide different insights. Wildfire distribution can reveal persistent hotspots and frequent fire activity, while smoke plume distribution is essential for assessing correlations with health impacts. Analyzing both datasets together enhances understanding of regional air quality and supports the development of smoke forecast models. However, comparing these disparate features without appropriate scaling and context can lead to spatial mis-contextualization, where localized patterns or anomalies may be obscured, potentially resulting in incorrect interpretations of their interrelationships. Identifying the optimal scale for analysis — whether for correlation or hotspot detection — is not always straightforward, underscoring the need for data solutions that support multi-scale analysis [Manley, 2021]. Discretizing large-scale vector features by decomposing them into varying resolutions of S2 cells can help reveal critical relationships and patterns that may be obscured at other scales.

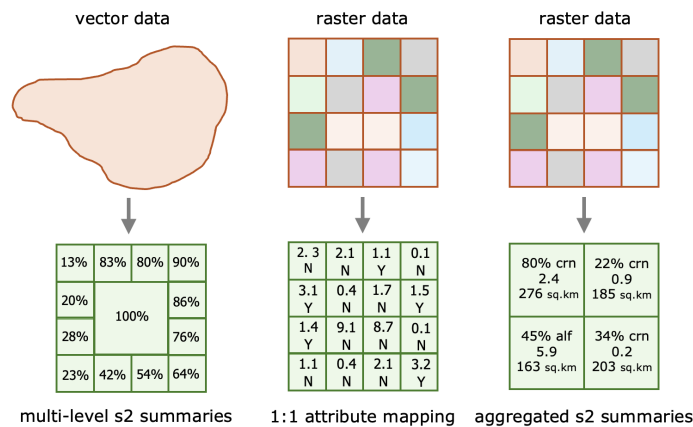


Figure 11: Examples of discretizing raster and vector data on the S2 grid.

Non-DGGS data can also be aggregated on the S2 grid as summaries (e.g., kernel density, spatial statistics, histograms, frequency transformations) to offer insights into aggregated spatial patterns without necessitating the retention of detailed individual records. Aggregation can occur at different levels of spatial granularity. For instance, real-time fire data can be aggregated at fine spatial scales (e.g., neighborhood or street levels) to facilitate targeted response efforts and resource allocation within localized areas. Aggregating the same fire data at higher spatial levels (e.g., city or county levels) helps in understanding broader phenomena such as air pollution or regional fire trends. Summaries computed at a lower level can be aggregated upward through the S2 hierarchy to compute values for larger spatial regions. Summaries can also be decomposed downward within the hierarchy, provided the feature in consideration is either `kwg-ont:sfEqual` or `kwg-ont:sfWithin` in the S2 cell at the top level. This hierarchical approach supports adaptive analysis, where users can dynamically adjust the level of decomposition to focus on specific spatial features or patterns of interest.

Both data decomposition and aggregation through discretization facilitate multi-scale analysis for both spatial and non-spatial dimensions of the data. The specific choice of method and selected grid resolution should reflect both the purpose and scale of the analysis. The hierarchical grid structure of S2 supports seamless transitions between different scales — from local to global — allowing for detailed representation and the discovery of patterns that may not be evident at a single scale. Furthermore, this quantization method improves data management by supporting feature simplification. It also supports advanced geovisualization techniques, allowing for dynamic scaling and context-aware rendering. This ensures that large-scale patterns and localized details are preserved and accurately represented, enhancing the ability to uncover meaningful spatial relationships and insights.

Here we describe two examples of data discretization in KWG: one for a vector dataset and another for a raster dataset.

4.2.1 Vector Data to S2 Cell Discretization

The Soil Survey Geographic Database¹⁷ (SSURGO) contains detailed information on hundreds of soil attributes, including chemical and physical properties, as well as their derived interpretations. The dataset comprises over 36 million soil map units distributed across more than 70 shapefiles, with varying scales depending on the region. For example, states like Nevada and Utah have large polygons mapped at a scale of 1:63,360, while agriculturally intensive states like Indiana and Iowa have finer polygons at a scale of 1:12,000. Due to its size and complexity, SSURGO data can be impractical for use in integrated analytics environments. In KWG, this dataset is decomposed onto the S2 reference cells. Figure 12 demonstrates the ontology pattern employed. Overlap areas between individual soil polygons and an S2 reference cell (measured in square kilometers) are precomputed and materialized as instances of the `kwg-ont:SoilMapUnitS2OverlapObservation` class, with the S2 cell serving as the feature of interest. The geometries of the original soil map units, represented by the `kwg-ont:SoilMapUnit` class, are also included in the graph along with the associated soil attributes, modeled as `kwg-ont:SoilMapUnitObservableProperty`. These geometries enable more accurate visualizations, as a single S2 cell can contain disconnected geometries from a soil multipolygon. Through the composition of relationships, `kwg-ont:overlapObservedWith` \circ `sosa:isFeatureOfInterestOf`, users can efficiently explore all soil properties linked to an S2 cell without the need to directly access soil polygon geometries. By discretizing soil data over a high-resolution S2 grid, the level of detail and accuracy is enhanced, allowing for integration with other thematic datasets such as landforms, floodplains, crop types, and high-resolution digital elevation models.

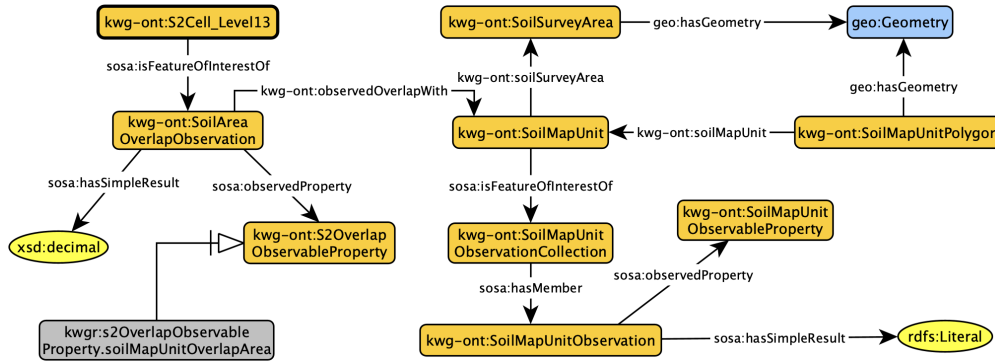


Figure 12: Ontology pattern for discretizing vector soil data from SSURGO to S2 reference cells.

To discretize SSURGO data, we build upon the method for computing topological relationships between vector geometries and S2 cells, as outlined in Section 4.1. Vector geometries of `kwg-ont:SoilMapUnitPolygon` geometries are approximated as `S2Polygon` objects, and their cell coverings are generated using S2 reference cells. The overlaps between the cells in the covering and the `S2Polygon` are computed using the `S2Polygon.GetOverlapFractions` method, which returns the fractional overlap of each cell relative to the polygon. This fraction is then multiplied by the cell’s area to compute the actual overlapping area on the Earth’s surface. This quantifiable measure allows for a more detailed understanding of soil properties associated with reference S2 cells.

4.2.2 Raster Data to S2 Cell Discretization

The USDA National Agricultural Statistics Service Cropland Data Layer¹⁸ (CDL) is a raster-based land cover dataset produced annually using satellite imagery and extensive agricultural ground reference data. The dataset has a ground resolution ranging from 30 to 56 meters, depending on the state and year. It tracks changes in forest extent and height, cropland, built-up areas, surface water, perennial snow and ice, and over 134 distinct crop types, making it highly valuable for monitoring agricultural land use in KWG. To integrate this data into KWG, the pixel-based raster information is transformed into data values representing the areal extent of each crop type within an S2 reference cell. Figure 13 illustrates the ontology pattern for this materialization in the graph. The areal percentage of each crop type within a reference cell, modeled as `kwg-ont:CroplandObservableProperty`, is computed and materialized as a temporally scoped observation instance of `kwg-ont:CroplandS2OverlapObservation`. To ensure data accuracy, we verify that the sum of all land cover observations within each cell, for a given timestamp, equals 100%. This discretization process reduces the large volume of raster CDL data and represents it in the graph, facilitating more

¹⁷<https://websoilsurvey.nrcs.usda.gov/app/WebSoilSurvey.aspx>

¹⁸<https://croplandcros.scinet.usda.gov/>

efficient and scalable computations. As a result, queries are attribute-based rather than spatial, improving both performance and manageability.

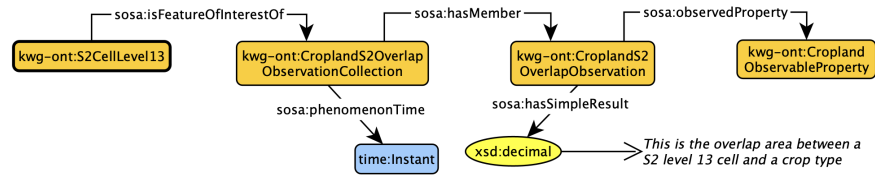


Figure 13: Ontology pattern for discretizing raster cropland data from USDA CDL to S2 reference cells.

The discretization of cropland data with S2 reference cells involves transforming raster representations into S2-compatible geometries to analyze spatial relationships more efficiently. Raster data is typically associated with a specific CRS, which must be transformed to align with the spherical geometry of the S2 library before generating S2 cell coverings and overlap calculations. The process begins by extracting the spatial bounds of the raster dataset from its metadata and defining the geographical coordinates of its corners. These bounds are then converted into an `S2Polygon`, which represents the geographical area covered by the raster on the spherical Earth. This conversion ensures the raster’s spatial footprint is accurately mapped onto the spherical surface for further analysis. Once the `S2Polygon` is established, the `S2RegionCoverer` method is used to cover the polygon with S2 reference cells. For each S2 cell in the covering, the raster values within the cell are aggregated to compute statistical summaries, such as the mean, sum, or other metrics relevant to the data. These statistical summaries provide quantifiable measures of the raster data’s distribution within each S2 cell.

5 Analytical Capabilities in KnowWhereGraph With S2 Integration

This section presents four use cases that demonstrate how the two quantization strategies enhance the analytical pipeline in KWG by optimizing storage and computation, while improving spatial query efficiency over heterogeneous datasets.

5.1 Conflating S2 Cells with Thematic Observation Data via Object Property Paths

Observation data, such as hurricane severity and impacts, population demographics, air quality indices, and public health observations, are collected through explicit or implicit sampling strategies. These datasets contain regional identifiers (e.g., ZIP code, FIPS code, NWZ code, statistical area code) but are not explicitly connected to region geometries. In KWG, these georeferenced observation data are linked to their corresponding geographic entities or regions, such as ZIP code tabulation areas, administrative region boundaries, national weather zones, and statistical areas, via the `sosa:hasFeatureOfInterest` relation as shown in Figures 14 and 15a.

From a query performance perspective, using S2 cells to topologically enrich geographic entities with explicit geometries is highly beneficial. This approach consequentially conflates S2 cells with various observation data via object property paths, thereby thematically contextualizing the cells. Figure 14 shows an example of the property path from various observations to S2 cells via connected geographic regions. The result of this process is a set of mappings from observations to geographic entities to sets of S2 cells at multiple levels of the S2 grid. This thematic enrichment of S2 cells entails a level of abstraction determined by the chosen geographic region and the resolution of the cells. However, it plays a crucial role in uncovering latent patterns, for example identifying that regions with high social vulnerability scores have an increased exposure to air pollution.

Figure 2 illustrates the ontology pattern that explicitly links observations to geographic regions using the `sosa:hasFeatureOfInterest` relation. The path between observations and S2 cells is defined using OWL 2 property chains [Potoniec, 2022], specifically through the composition of `sosa:hasFeatureOfInterest` and `kgw-ont:sfOverlaps`. In KWG, these object paths are computed on-demand via SPARQL queries.

Thematic contextualization of S2 cells provides significant advantages for use cases requiring granular spatial summarization, cross-theme data exploration, and spatial interpolation. Conflating different observational themes with S2 cells enables users to navigate geographically through thematic data spaces. This is especially valuable for locating related places within the knowledge graph. For example, an analyst from a humanitarian aid organization may search for regions based on thematic criteria, such as identifying S2 cells associated with fire forecasts, weather conditions conducive to fires, and socioeconomically vulnerable neighborhoods. This integrated data approach assists the analyst in developing effective emergency response plans. Figure 3a illustrates the SPARQL query used to retrieve this information

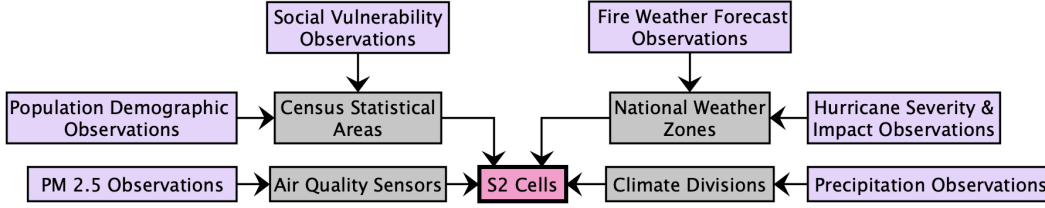


Figure 14: This figure illustrates the contextual enrichment of S2 cells with various observational data via geographic entities in KWG. Purple boxes represent observation data, while grey boxes denote geographic features with explicit geometries. Arrows indicate the linkages connecting observations to features and, in turn, to the corresponding S2 cells.

from KWG. Additionally, thematic conflation supports advanced geo-visualization techniques, allowing for dynamic representation of hotspots or areas of interest at different zoom levels, essential for detailed spatial analysis and informed decision-making.

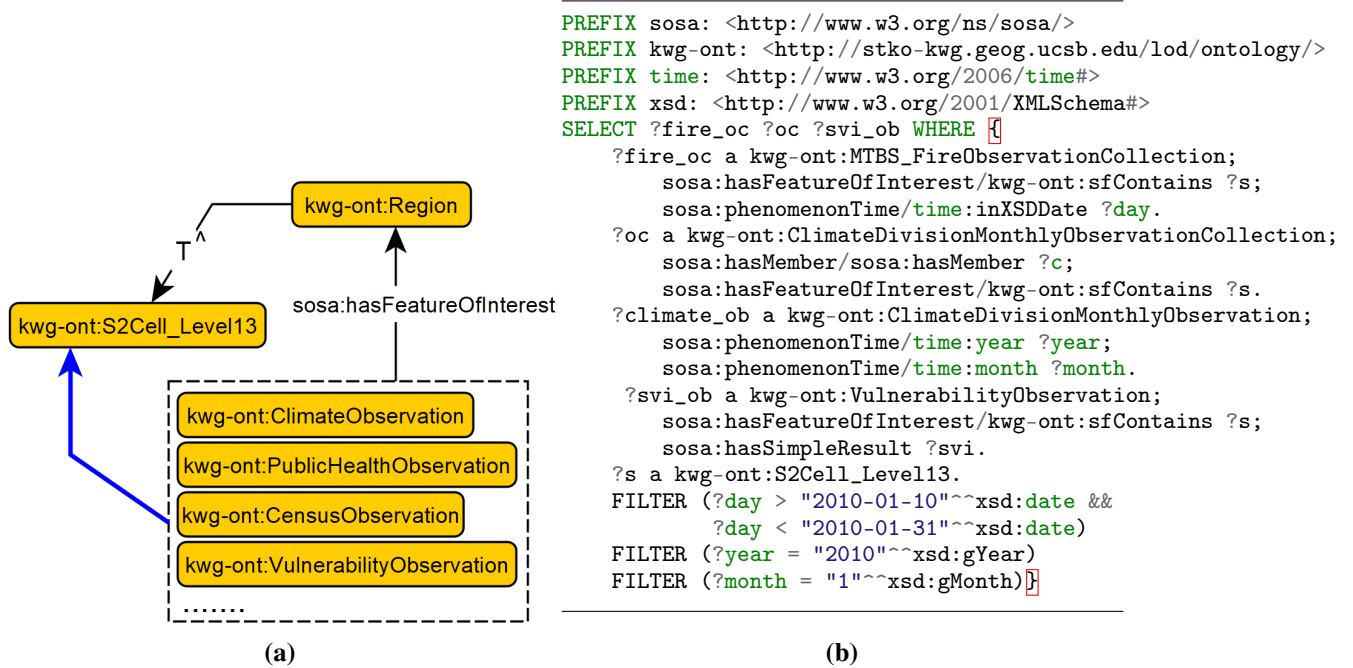


Figure 15: (a) Pattern for conflating observation data on S2 cells via object property paths. The blue arrow denotes the shortcut that can be computed on demand with dedicated SPARQL queries or materialized via ontology rules. (b) Sample SPARQL query to identify S2 level 13 cells linked to fire risk during January 2010.

5.2 Multi-scale Representation of Quantitative Geospatial Data

Quantitative datasets consist of various observation datasets typically represented as numerical values associated with specific locations. Examples include the Social Vulnerability Index (SVI) linked to counties and PM 2.5 concentrations measured at point-based air quality monitoring sites. While these datasets can be queried through conflation at specific S2 grid levels, some statistical queries may not benefit from a multi-scale spatial representation. This largely depends on the type of quantity (amounts versus measurements, as discussed in [Top, 2024]). For instance, while a county-level SVI measurement can be mapped to all S2 reference cells within that county, these values cannot simply be summed or averaged to derive a value for a larger spatial region, such as a state. In contrast, the spatial overlap areas of a specific crop type from multiple S2 cells can be summed to determine the total overlap area within a larger S2 cell that contains them. The distinction between quantities that can be aggregated (mereotopological quantities) and those that

cannot (arithmetic quantities) is further defined and axiomatized in [Top, 2024]. While discussing the implications of discretizing both types of quantities and their aggregations over multiple resolutions is beyond the scope of this paper, understanding these distinctions is crucial for accurate geospatial analysis and data integration within the S2 Geometry framework.

When aggregating certain quantity measurements over a larger region, it is important to incorporate weighting measures to adjust for spatial biases or the uneven distribution of data points within that region. For example, an averaging query that requests the mean of data values within a specified spatial polygon can benefit from information regarding the S2 cell containing each data point, its spatial relationship to the polygon, and the size of the S2 cell. These details help determine how data points are placed within the polygon and the appropriate weights to allocate. By incorporating these weighting factors, the aggregated results may more accurately reflect the true characteristics of the entire area, rather than being skewed by the concentration or distribution of the data points. A key objective in defining such a representation is to facilitate queries at the data’s coarse scale without significant loss of accuracy.

Consider the air quality observation dataset in KWG, which contains concentration measurements for pollutants such as Ozone and PM 2.5. The PM 2.5 concentration is a critical metric in air quality assessment. Typically, air quality monitoring sites are associated with counties, but their distribution within counties is neither uniform nor evenly spaced. This uneven distribution complicates the derivation of accurate county-level estimates since PM 2.5 concentrations exhibit nonlinear spatial variations. For example, urban areas require data with a spatial resolution of 200 - 400 meters to achieve acceptable modeling accuracy of pollution exposure [Stroh et al., 2007]. In KWG, individual PM 2.5 measurements are mapped onto 1 x 1 km² grid cells represented by S2 reference cells. These measurements are then hierarchically contained within lower-resolution S2 cells, which are also topologically connected to county polygon boundaries through spatial quantization. This hierarchical structuring enables users to analyze the spatial distribution of monitoring sites within counties, facilitating the calculation of appropriate weights for more accurate regional estimates. This hierarchical structuring helps users analyze the distribution of monitoring sites within counties and calculate weights for more accurate regional estimates. It accounts for the uneven density of monitoring sites, their proximity to pollution sources, and any spatial biases from uneven observation distribution. Moreover, the fine-grained overlap of monitoring sites with other data layers – achieved through S2 enrichment and discretization – enhances the ability to identify additional controlling factors or measures that may disproportionately influence PM 2.5 concentrations at specific locations. Thus, the combination of quantization and the hierarchical and topological relationships within the S2 grid framework significantly improves the precision and reliability of aggregating quantities over spatial scales, particularly in regions with complex spatial characteristics.

5.3 Cross-Graph Integration

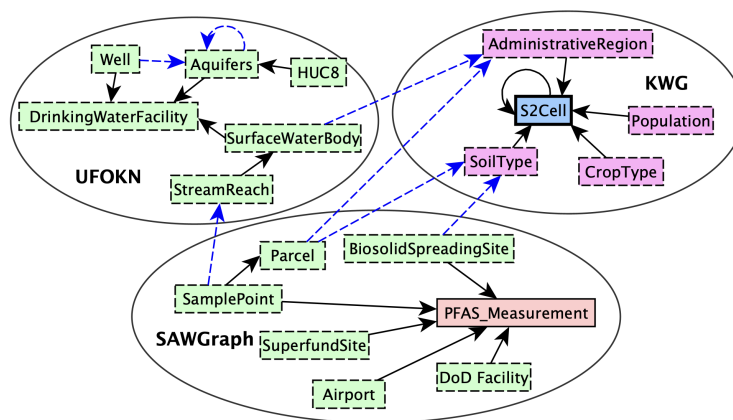


Figure 16: Overview of cross-integration between KWG, SAWGraph, and UFOKN. Pink boxes represent concepts from KWG linked to S2 cells. Solid black arrows depict prematerialized links in the graph. Green boxes, representing concepts from UFOKN and SAWGraph, are directly associated with S2 cells and conflated with other spatial and thematic concepts, as shown by the blue dashed arrows. These arrows illustrate object property paths that can be queried via SPARQL queries.

S2 serves as the *spatial fabric* for cross-disciplinary graph integration and interoperability within the OKN framework, which includes SAWGraph and UFOKN, as outlined in Section 2. SAWGraph integrates datasets related to water, soil, plant and animal tissue, feed, and agricultural food products tested for per- and polyfluoroalkyl substances (PFAS), covering test results, testing locations, and potential contamination sources. This integration supports the analytical

needs for PFAS monitoring and management. SAWGraph is connected with KWG and UFOKN to trace PFAS transport and accumulation pathways within the U.S. food and water systems, and to prioritize further sampling at specific locations, such as wells, agricultural lands, or crops, using federated querying with S2 cells as points of interest. To enable such functionality, each graph must implement S2 integration with relevant datasets. Figure 16 illustrates key spatial features from each graph that are linked to S2 cells via topological enrichment, enabling the contextualization and conflation of datasets by leveraging complementary information across graphs. Inferred links (depicted with dashed blue arrows) allow for advanced queries, such as: “*What is the relationship between PFAS releases from paper mills and PFAS test results in nearby or downstream water bodies*”. Figure 17 shows a map demonstrating how spatial data from the three graphs are integrated and utilized in this context. This integrated spatial framework enhances the ability to conduct cross-regional comparisons and make informed decisions regarding contamination and sampling priorities.

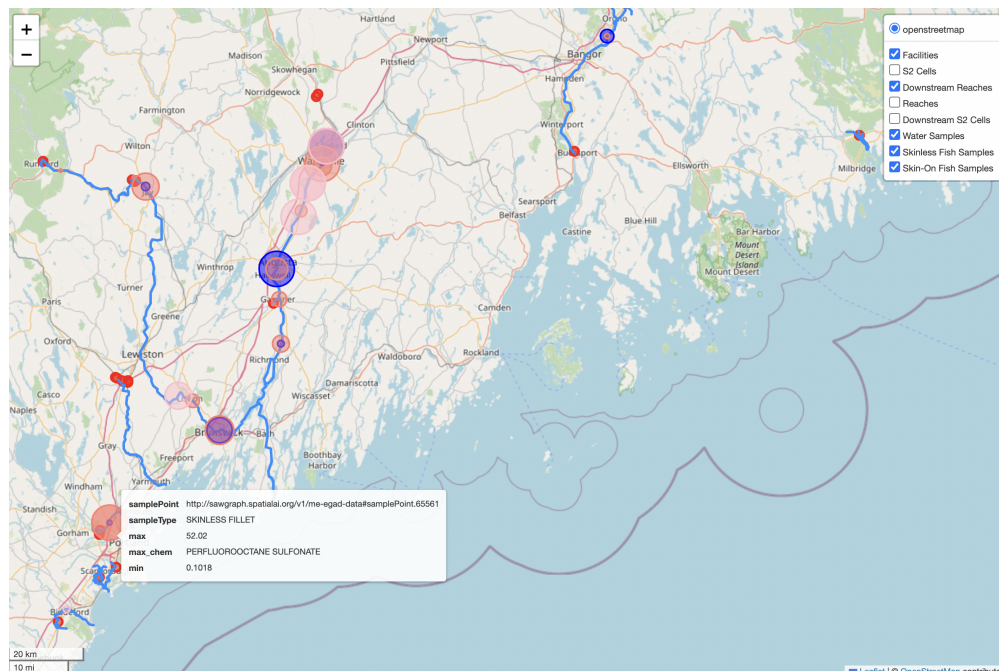


Figure 17: Screenshot of the map showing the locations of paper mills, the volume of PFAS releases, and PFAS test results in nearby or downstream water bodies and fish tissue samples. Test values are aggregated by sample location, highlighting the lowest and highest PFAS concentrations at each point. S2 cells are used to perform spatial queries, identifying locations upstream and downstream from each sample point. The Python notebook that demonstrates this query is available in this Github repository: <https://github.com/shirlysteph/s2-kwg/tree/main/demos/cross-graph>

5.4 Graph Sharding

KWG is a continuously expanding knowledge graph, with the number of geometry nodes increasing significantly - from approximately 5.5 million in version 2.0 (KWG - Manhattan) to approximately 48 million in version 3.0 (KWG - Santa Barbara). This growth is expected to continue, necessitating careful consideration of scalability for both maintenance and performance. Managing such large volumes of data introduces challenges not only for efficient search but also for data ingestion, indexing, and updating, especially as highly dynamic environmental datasets are integrated into the graph. To mitigate the challenges posed by the increasing size, the graph can be partitioned into smaller sub-graphs or shards, which can be distributed across a cluster of servers for parallel processing. This approach leverages distributed computing to manage both the storage and query processing loads. Federated SPARQL queries can then be executed to aggregate results from the distributed shards, enabling efficient querying across the graph’s full dataset while maintaining scalability and performance [W3C, 2021].

Several sharding approaches exist, with the appropriate method depending on factors like query patterns and data characteristics [Saleem et al., 2023]. For KWG, where the focus is on spatial insights, location-based sharding is a viable strategy, assuming spatial affinity between queries and specific regions [Ren F and Thomson D, 2018]. For instance, queries might focus on population health and public health facilities in hurricane-affected areas. However,

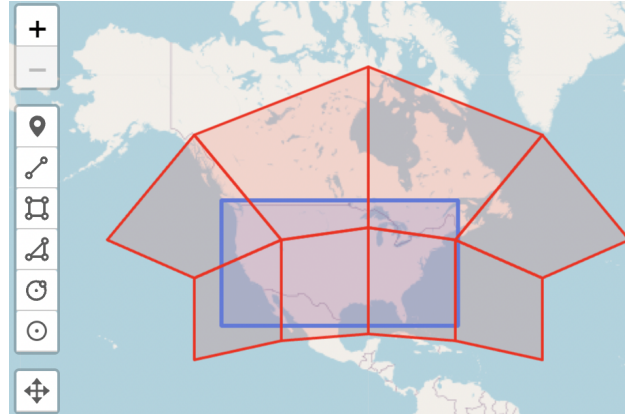


Figure 18: Eight S2 cells at level 2, drawn in red, overlap the continental U.S.

in a complex GeoKG like KWG, where data often spans flat geographic boundaries (e.g., natural phenomena like wildfires), a purely region-based sharding approach may be insufficient. To address this, sharding should partition data in geographies with minimal cross-region interaction, reducing distributed joins during federated queries and improving efficiency while preserving spatial relationships. Geospatial data in KWG is already clustered on the S2 grid using topological indexing, conflation, and quantization, making the S2 grid a natural choice for location-based partitioning. Data from different S2 cells (at an appropriate level) can be distributed across servers, forming a cluster of shards further indexed (e.g., using Elasticsearch). For example, sharding North American data on the S2 grid at level 2 results in eight servers corresponding to the eight S2 cells overlapping the region – see Figure 18. Shard routing algorithms, like those in Elasticsearch, can then direct federated queries to the appropriate server.

6 Conclusion

This paper demonstrates how the implementation of S2 Geometry using GeoSPARQL’s vector data model as an RDF graph establishes the DGGS as a versatile spatial data reference framework. This integration enhances the functionality of GeoKG infrastructures by eliminating the need for specialized geographic extensions typically required for raster and gridded data representation. By utilizing well-supported Simple Feature geometry types and optimized geometry serializations like WKT and GML, the integration process for heterogeneous data is streamlined. The connectivity and hierarchical relationships between S2 cells, established using GeoSPARQL’s topological relations, enhance the qualitative spatial perception of the S2 RDF graph. This approach simplifies the querying of complex spatial data, reducing the need for combined vector/raster querying through cross-geometric operations and raster functions, such as raster algebra operations constructed in GeoSPARQL+ [Homburg et al., 2020], by instead enabling efficient execution of spatial operations such as basic SPARQL and GeoSPARQL functions.

In the KWG framework, we have successfully implemented quantization methods that treat S2 cells as vector bins for encapsulating both qualitative and quantitative geospatial information. By pre-materializing statements for this binning as RDF triples, we optimize performance for computationally expensive queries involving spatial predicates or join operations. Instead of scanning the entire graph, these queries can swiftly access relevant materialized views associated with specific S2 cells, resulting in significant improvements in query response times. Specifically, the discretization process transforms spatial data into a finer, more granular format directly linked to S2 cells, allowing for effective representation and querying of remotely sensed raster environmental observation data, which graph databases are not fully fledged to handle.

Furthermore, the geometric and semantic flexibility of the S2 RDF graph facilitates spatial graph analytics through cell-based raster-to-vector conflation. The hierarchical structure of S2 grids, along with explicit relationships between cells at different resolutions, allows for consistent multi-resolution data representation and integration of time-series geospatial data. However, we acknowledge that discretization must be approached with caution; the results’ quality is highly contingent upon the original data accuracy, spatial uncertainty, and area distortion associated with each cell. By cross-linking various thematic datasets in KWG via stable, portable S2 cell identifiers, we support efficient data representation by potentially rendering some geometries redundant.

The modular data model inherent in S2 promotes flexible and efficient data management, ensuring scalability and sustainability in graph maintenance. This structure enables straightforward partitioning of spatial data, which is

especially advantageous in distributed computing environments for processing large-scale geospatial datasets through parallel processing techniques. Grid cells serve as analytic tiles, facilitating client-side analytics such as machine learning model development and geovisualization.

Transforming and representing non-DGGS spatial data within a DGGS framework requires a deep understanding of the specific DGGS software library being utilized. Due to the size and complexity of geospatial datasets, particularly when dealing with intricate polygon geometries, quantization can require substantial computational power and processing time, potentially leading to oversimplifications of the original data. The prevalent use of geographic CRS such as WGS84 and EPSG:4326 in traditional geospatial workflows complicates the accurate handling of spherical geometries like those used by the S2 library. Accurate conversion between common geographic CRS and spherical representations is critical, particularly when dealing with large spatial extents, as transitioning from vector or raster formats to DGGS cells can lead to data loss or inaccuracies. Moreover, the variable resolution of DGGS cells can introduce issues such as the Modifiable Areal Unit Problem, as not all S2 cells are equal-area at each level. When discretizing information onto S2 cells, it is essential to carefully quantify and express spatial uncertainty, especially when working across multiple scales. While encoding spatial uncertainty within DGGS cells enhances the overall accuracy of geospatial analytics, it also introduces complexities for decision-makers who are accustomed to working with traditional raster and vector formats. Moreover, this shift raises important questions about how DGGS impacts multiscale analysis and its suitability for decision-making workflows that rely on high-fidelity geographic data.

This paper outlines a comprehensive methodological framework for leveraging S2 Geometry as an integration framework, enabling the semantic reconciliation and fusion of diverse vector and raster datasets across multiple spatial scales and CRS. By addressing the limitations of traditional graph databases in handling complex geospatial data, our approach introduces quantization techniques within KWG that are tailored to specific analytical use cases. These methods not only data accessibility but also support a broader vision of advanced spatial analytics within the context of GeoKGs. While we acknowledge current challenges – such as spatial uncertainty and computational scalability – our goal is to foster collaboration within the geographic information science research community by presenting critical open questions. This dialogue is essential for advancing more accurate, integrated geospatial analyses and fostering innovation within the evolving GeoKG landscape.

References

- Pascal Hitzler. A review of the Semantic Web field. *Commun. ACM*, 64(2):76–83, 2021. URL <https://doi.org/10.1145/3397512>.
- Shaoxiong Ji, Shirui Pan, Erik Cambria, Pekka Marttinen, and S Yu Philip. A survey on Knowledge Graphs: Representation, acquisition, and applications. *IEEE transactions on neural networks and learning systems*, 33(2):494–514, 2021.
- Bilal Abu-Salih. Domain-specific Knowledge Graphs: A survey. *Journal of Network and Computer Applications*, 185: 103076, 2021.
- Mark D Wilkinson, Michel Dumontier, IJsbrand Jan Aalbersberg, Gabrielle Appleton, Myles Axton, Arie Baak, Niklas Blomberg, Jan-Willem Boiten, Luiz Bonino da Silva Santos, Philip E Bourne, et al. The FAIR guiding principles for scientific data management and stewardship. *Scientific data*, 3(1):1–9, 2016.
- Krzysztof Janowicz, Pascal Hitzler, Wenwen Li, Dean Rehberger, Mark Schildhauer, Rui Zhu, Cogan Shimizu, Colby Fisher, Ling Cai, Gengchen Mai, et al. Know, Know Where, KnowWhereGraph: A densely connected, cross-domain knowledge graph and geo-enrichment service stack for applications in environmental intelligence. *AI Magazine*, 43(1):30–39, 2022.
- J Michael Johnson, Tom Narock, Justin Singh-Mohudpur, Doug Fils, Keith Clarke, Siddharth Saksena, Adam Shepherd, Sankar Arumugam, and Lilit Yeghiazarian. Knowledge Graphs to support real-time flood impact evaluation. *AI Magazine*, 43(1):40–45, 2022.
- Bo Yan, Gengchen Mai, Yingjie Hu, and Krzysztof Janowicz. Harnessing heterogeneous big geospatial data. In *Handbook of Big Geospatial Data*, pages 459–473. Springer, 2020.
- Frank Manola, Eric Miller, Brian McBride, et al. RDF primer. *W3C recommendation*, 10(1-107):6, 2004.
- Nicholas J Car and Timo Homburg. GeoSPARQL 1.1: Motivations, details and applications of the decadal update to the most important geospatial LOD standard. *ISPRS International Journal of Geo-Information*, 11(2):117, 2022.
- Krzysztof Janowicz, Kitty Currier, Cogan Shimizu, Rui Zhu, Meilin Shi, Colby K Fisher, Dean Rehberger, Pascal Hitzler, Zilong Liu, and Shirly Stephen. Fast forward from data to insight: (Geographic) Knowledge Graphs and their applications. In *Handbook of Geospatial Artificial Intelligence*, pages 411–426. CRC Press, 2023.

- Milos Jovanovik, Timo Homburg, and Mirko Spasić. A GeoSPARQL compliance benchmark. *ISPRS International Journal of Geo-Information*, 10(7):487, 2021.
- Weiming Huang, Syed Amir Raza, Oleg Mirzov, and Lars Harrie. Assessment and benchmarking of spatially enabled RDF stores for the next generation of spatial data infrastructure. *ISPRS International Journal of Geo-Information*, 8(7):310, 2019.
- Konstantinos Theocharidis, John Liagouris, Nikos Mamoulis, Panagiotis Bouros, and Manolis Terrovitis. SRX: efficient management of spatial RDF data. *The VLDB Journal*, 28:703–733, 2019.
- Ravi Kanth V Kothuri, Siva Ravada, and Daniel Abugov. Quadtree and R-tree indexes in oracle spatial: a comparison using GIS data. In *Proceedings of the 2002 ACM SIGMOD international conference on Management of data*, pages 546–557, 2002.
- Abhirup Acharya. How companies like Uber, Google and Airbnb disrupt industries with location intelligence?, 2023. URL <https://medium.com/@abhirup.acharya009/how-companies-like-uber-google-and-airbnb-disrupt-industries-with-location-intelligence-f4fb6ddc3808>.
- Wenwen Li, Sizhe Wang, Sheng Wu, Zhining Gu, and Yuanyuan Tian. Performance benchmark on semantic web repositories for spatially explicit knowledge graph applications. *Computers, environment and urban systems*, 98:101884, 2022a.
- David Manley. Scale, aggregation, and the modifiable areal unit problem. In *Handbook of regional science*, pages 1711–1725. Springer, 2021.
- Frank Davis, Dalea Quattrochi, Merrilck Ridd, Ninas Lam, Stephen J Walsh, Joel C Michaelsen, Janet Franklin, Douglas A Stow, Chris J Johannsen, and Carol A Johnston. Environmental analysis using integrated GIS and remotely sensed data – Some research needs and priorities. *Photogrammetric Engineering and Remote Sensing*, 57(6):689–697, 1991.
- Kevin Sahr, Denis White, and A Jon Kimerling. Geodesic Discrete Global Grid Systems. *Cartography and Geographic Information Science*, 30(2):121–134, 2003.
- MF Goodchild. Geographical grid models for environmental monitoring and analysis across the globe (panel session). In *Proceedings of GIS/LIS'94 Conference*, 1994.
- Mingke Li and Emmanuel Stefanakis. Geospatial operations of discrete global grid systems – A comparison with traditional GIS. *Journal of Geovisualization and Spatial Analysis*, 4(2):26, 2020.
- Majid Hojati, Colin Robertson, Steven Roberts, and Chiranjib Chaudhuri. GIScience research challenges for realizing discrete global grid systems as a Digital Earth. *Big Earth Data*, 6(3):358–379, 2022.
- Ben Bondaruk, Steven A Roberts, and Colin Robertson. Assessing the state of the art in Discrete Global Grid Systems: OGC criteria and present functionality. *Geomatica*, 74(1):9–30, 2020.
- Ali Mahdavi-Amiri, Troy Alderson, and Faramarz Samavati. A survey of digital earth. *Computers & Graphics*, 53:95–117, 2015.
- Colin Robertson, Chiranjib Chaudhuri, Majid Hojati, and Steven A Roberts. An integrated environmental analytics system (IDEAS) based on a DGGS. *ISPRS Journal of Photogrammetry and Remote Sensing*, 162:214–228, 2020.
- Xiaochuang Yao, Guoqing Li, Junshi Xia, Jin Ben, Qianqian Cao, Long Zhao, Yue Ma, Lianchong Zhang, and Dehai Zhu. Enabling the big earth observation data via cloud computing and DGGS: Opportunities and challenges. *Remote Sensing*, 12(1):62, 2019.
- OGC. Topic 21: Discrete Global Grid Systems abstract specification., 2017. URL <http://docs.opengeospatial.org/as/15-104r5/15-104r5.html>.
- E Veach, J Rosenstock, E Engle, and T Manshreck. S2 Geometry Library: Computational geometry and spatial indexing on the sphere. *Software*, 2017. URL <http://s2geometry.io/>.
- Uber. Uber H3: a hexagonal hierarchical geospatial indexing system. Release: 4.1.0, 2023. URL <https://github.com/uber/h3>.
- RG Gibb. The rHEALPix Discrete Global Grid System. In *IOP Conference Series: Earth and Environmental Science*, volume 34, page 012012. IOP Publishing, 2016.
- Riskaware Ltd. OpenEAGGR: Open Equal Area Global GRid. Release: 2.0, 2017. URL <https://github.com/riskaware-ltd/open-eaggr>.
- Mingke Li, Heather McGrath, and Emmanuel Stefanakis. Integration of heterogeneous terrain data into Discrete Global Grid Systems. *Cartography and Geographic Information Science*, 48(6):546–564, 2021.

- Bart Kranstauber, Rolf Weinzierl, Martin Wikelski, and Kamran Safi. Global aerial flyways allow efficient travelling. *Ecology letters*, 18(12):1338–1345, 2015.
- Andrey N Romanov and Ilya V Khvostov. Emissivity peculiarities of the inland salt marshes in the south of Western Siberia. *International journal of remote sensing*, 39(2):418–431, 2018.
- Rafael HM Pereira, Daniel Herszenhut, Marcus Saraiva, and Steve Farber. Ride-hailing and transit accessibility considering the trade-off between time and money. *Cities*, 144:104663, 2024.
- Bingxian Lin, Liangchen Zhou, Depeng Xu, A-Xing Zhu, and Guonian Lu. A Discrete Global Grid System for earth system modeling. *International Journal of Geographical Information Science*, 32(4):711–737, 2018.
- Michael F. Goodchild. Reimagining the history of GIS. *Annals of GIS*, 24(1):1–8, 2018.
- Irina Bastrakova and Shane Crossman. Enabling communities to integrate earth, space and environmental data - Australian Location Index. *Earth and Space Science Open Archive ESSOAr*, 2020.
- Nicholas J. Car Car, Timo Homburg, Matthew Perry, Frans Knibbe, Simon J.D. Cox, Joseph Abhayaratna, Mathias Bonduel, Paul J. Cripps, and Krzysztof Janowicz. OGC GeoSPARQL – A geographic query language for RDF data, 2023. URL <http://www.opengis.net/doc/IS/geosparql/1.1>.
- David Habgood, Timo Homburg, Nicholas J Car, and Milos Jovanovik. Implementation and compliance benchmarking of a DGGS-enabled, GeoSPARQL-aware triplestore. In *Proceedings of the 5th International Workshop on Geospatial Linked Data co-located with ESWC, May 30 2022, Hersonissos, Greece, 2022*.
- Vikram Gundeti. Introducing the Foursquare graph, a pioneer in location intelligence, 2023. URL <https://location.foursquare.com/resources/blog/capabilities/knowledge-graph-technology/>.
- Joseph Zalewski, Pascal Hitzler, and Krzysztof Janowicz. Semantic compression with region calculi in nested hierarchical grids. In *Proceedings of the 29th International Conference on Advances in Geographic Information Systems*, pages 305–308, 2021.
- Max J Egenhofer, David M Mark, and John Herring. The 9-intersection: Formalism and its use for natural-language spatial predicates (94-1). *NCGIA Technical Reports*, 1994.
- Krzysztof Janowicz, Armin Haller, Simon JD Cox, Danh Le Phuoc, and Maxime Lefrançois. SOSA: A lightweight ontology for sensors, observations, samples, and actuators. *Journal of Web Semantics*, 56:1–10, 2019.
- Markos K Iliakis. Geospatial Query Answering Using Knowledge Graph Embeddings. 2022.
- Rui Zhu, Shirly Stephen, Lu Zhou, Cogan Shimizu, Ling Cai, Gengchen Mai, Krzysztof Janowicz, Pascal Hitzler, and Mark Schildhauer. Environmental observations in Knowledge Graphs. In *DaMaLOS*, pages 1–11, 2021a.
- Bingchuan Jiang, Xiong You, Ke Li, Tingting Li, Xiaojun Zhou, and Liheng Tan. Interactive analysis of epidemic situations based on a spatiotemporal information knowledge graph of COVID-19. *IEEE Access*, 10:46782–46795, 2020.
- Rui Zhu, Krzysztof Janowicz, Gengchen Mai, Ling Cai, and Meilin Shi. COVID-forecast-graph: An open Knowledge Graph for consolidating COVID-19 forecasts and economic indicators via place and time. *AGILE: GIScience Series*, 3:21, 2022a.
- Martin Böckling, Heiko Paulheim, and Sarah Detzler. A planet scale spatial-temporal Knowledge Graph based On OpenStreetMap and H3 Grid. *arXiv preprint arXiv:2405.15375*, 2024.
- Yanlin Qi, Gengchen Mai, Rui Zhu, and Michael Zhang. EVKG: An interlinked and interoperable electric vehicle Knowledge Graph for smart transportation system. *Transactions in GIS*, 27(4):949–974, 2023.
- Zhiheng Zhao, Mengdi Zhang, Jian Chen, Ting Qu, and George Q Huang. Digital twin-enabled dynamic spatial-temporal knowledge graph for production logistics resource allocation. *Computers & Industrial Engineering*, 171:108454, 2022.
- Gengchen Mai, Krzysztof Janowicz, Rui Zhu, Ling Cai, and Ni Lao. Geographic question answering: challenges, uniqueness, classification, and future directions. *AGILE: GIScience series*, 2:8, 2021.
- Georg Weinberger, Johannes Scholz, and Eveline Wandl-Vogt. Towards an intuitive user interface and geographic question answering for an existing spatial linked data endpoint for dialect data. *Abstracts of the ICA*, 5:1–3, 2022.
- Dániel Balla, Marianna Zichar, Róbert Tóth, Emőke Kiss, Gergő Karancsi, and Tamás Mester. Geovisualization techniques of spatial environmental data using different visualization tools. *Applied Sciences*, 10(19):6701, 2020.
- Wenwen Li, Sizhe Wang, Xiao Chen, Yuanyuan Tian, Zhining Gu, Anna Lopez-Carr, Andrew Schroeder, Kitty Currier, Mark Schildhauer, and Rui Zhu. GeoGraphVis: a Knowledge Graph and geovisualization empowered cyberinfrastructure to support disaster response and humanitarian aid. *ISPRS International Journal of Geo-Information*, 12(3):112, 2023.

- Rui Zhu, Krzysztof Janowicz, Ling Cai, and Gengchen Mai. Reasoning over higher-order qualitative spatial relations via spatially explicit neural networks. *International Journal of Geographical Information Science*, 36(11):2194–2225, 2022b.
- Gengchen Mai, Yingjie Hu, Song Gao, Ling Cai, Bruno Martins, Johannes Scholz, Jing Gao, and Krzysztof Janowicz. Symbolic and subsymbolic GeoAI: Geospatial Knowledge Graphs and spatially explicit machine learning. *Transactions in GIS*, 26(8):3118–3124, 2022.
- U.S. National Science Foundation. Open Knowledge Network: Creating the semantic information infrastructure for the future, November 2018. URL <https://www.nitr.gov/news/Open-Knowledge-Network-Workshop-Report-2018.asp>.
- Siddharth Saksena. Urban Flooding Open Knowledge Network (UF-OKN): Current products and future functionalities. In *AGU Fall Meeting Abstracts*, volume 2022, pages H46D–02, 2022.
- Pascal Hitzler, Markus Krötzsch, Bijan Parsia, Peter F Patel-Schneider, Sebastian Rudolph, et al. OWL 2 web ontology language primer. *W3C recommendation*, 27(1):123, 2009.
- Pascal Hitzler, Markus Krötzsch, and Sebastian Rudolph. *Foundations of Semantic Web technologies*. Chapman and Hall/CRC Press, 2010. ISBN 9781420090505. URL <http://www.semantic-web-book.org/>.
- World Wide Web Consortium and others. SPARQL 1.1 overview, 2013. URL <https://www.w3.org/TR/sparql11-query/>.
- Blake Regalia, Krzysztof Janowicz, and Grant McKenzie. Revisiting the representation of and need for raw geometries on the linked data web. In *LDOW@ WWW*, 2017.
- Philippe Rigaux, Michel Scholl, and Agnes Voisard. *Spatial databases: with application to GIS*. Morgan Kaufmann, 2002.
- Dimitris Papadias, Jun Zhang, Nikos Mamoulis, and Yufei Tao. Query processing in spatial network databases. In *Proceedings 2003 VLDB Conference*, pages 802–813. Elsevier, 2003.
- Parker Dinkins. Quad-tree geospatial data structure: functionality, benefits, and limitations, 2023. URL <https://opensourcegisdata.com/quad-tree-geospatial-data-structure-functionality-benefits-and-limitations.html>.
- Theofilos Ioannidis, George Garbis, Kostis Kyzirakos, Konstantina Bereta, and Manolis Koubarakis. Evaluating geospatial RDF stores using the benchmark Geographica 2. *Journal on Data Semantics*, 10(3):189–228, 2021.
- Blake Regalia, Krzysztof Janowicz, and Grant McKenzie. Computing and querying strict, approximate, and metrically refined topological relations in linked geographic data. *Transactions in GIS*, 23(3):601–619, 2019.
- Rui Zhu, Ling Cai, Gengchen Mai, Cogan Shimizu, Colby K Fisher, Krzysztof Janowicz, Anna Lopez-Carr, Andrew Schroeder, Mark Schildhauer, Yuanyuan Tian, et al. Providing humanitarian relief support through knowledge graphs. In *Proceedings of the 11th Knowledge Capture Conference*, pages 285–288, 2021b.
- Cogan Shimizu, Shirly Stephen, Rui Zhu, Kitty Currier, Mark Schildhauer, Dean Rehberger, Pascal Hitzler, Krzysztof Janowicz, Colby K Fisher, Mohammad Saeid Mahdavejad, et al. The KnowWhereGraph Ontology. *Under review*, 2023.
- Armin Haller, Krzysztof Janowicz, Simon JD Cox, Maxime Lefrançois, Kerry Taylor, Danh Le Phuoc, Joshua Lieberman, Raúl García-Castro, Rob Atkinson, and Claus Stadler. The modular SSN ontology: A joint W3C and OGC standard specifying the semantics of sensors, observations, sampling, and actuation. *Semantic Web*, 10(1):9–32, 2019.
- Krzysztof Janowicz. Observation-driven geo-ontology engineering. *Transactions in GIS*, 16(3):351–374, 2012.
- Ali Mahdavi Amiri, Troy Alderson, and Faramarz Samavati. Geospatial data organization methods with emphasis on aperture-3 hexagonal discrete global grid systems. *Cartographica: The International Journal for Geographic Information and Geovisualization*, 54(1):30–50, 2019.
- Vojtěch Uher, Petr Gajdoš, Václav Snášel, Yu-Chi Lai, and Michal Radecký. Hierarchical hexagonal clustering and indexing. *Symmetry*, 11(6):731, 2019.
- David Bowater and Emmanuel Stefanakis. On the isolatitude property of the rHEALPix Discrete Global Grid System. *Big Earth Data*, 3(4):362–377, 2019.
- Alexander Kmoch, Ivan Vasilyev, Holger Virro, and Evelyn Uuemaa. Area and shape distortions in open-source discrete global grid systems. *Big Earth Data*, 6(3):256–275, 2022.
- Michael F Goodchild. Discrete global grids for digital earth. In *International Conference on Discrete Global Grids*, pages 26–28. Citeseer, 2000.

- Robin Kraft, Ferdinand Birk, Manfred Reichert, Aniruddha Deshpande, Winfried Schlee, Berthold Langguth, Harald Baumeister, Thomas Probst, Myra Spiliopoulou, and Rüdiger Pryss. Design and implementation of a scalable crowdsensing platform for geospatial data of tinnitus patients. In *2019 IEEE 32nd International Symposium on Computer-Based Medical Systems (CBMS)*, pages 294–299. IEEE, 2019.
- Neeraj Sirdeshmukh, Edward Verbree, Peter van Oosterom, Stella Psomadaki, and Martin Kodde. Utilizing a Discrete Global Grid System for handling point clouds with varying locations, times, and levels of detail. *Cartographica: The International Journal for Geographic Information and Geovisualization*, 54(1):4–15, 2019.
- Paulo Raposo. Geovisualization of complex origin-destination flow maps using Discrete Global Grid Systems. *Abstracts of the ICA*, 1:1–3, 2019.
- Mingke Li, Heather McGrath, and Emmanuel Stefanakis. Geovisualization of hydrological flow in hexagonal grid systems. *Geographies*, 2(2):227–244, 2022b.
- Bernardo BN Strassburg, Annabel Kelly, Andrew Balmford, Richard G Davies, Holly K Gibbs, Andrew Lovett, Lera Miles, C David L Orme, Jeff Price, R Kerry Turner, et al. Global congruence of carbon storage and biodiversity in terrestrial ecosystems. *Conservation Letters*, 3(2):98–105, 2010.
- Andrew Rawson, Zoheir Sabour, and Mario Brito. Intelligent geospatial maritime risk analytics using the Discrete Global Grid System. *Big Earth Data*, 6(3):294–322, 2022.
- Justin Bousquin. Discrete Global Grid Systems as scalable geospatial frameworks for characterizing coastal environments. *Environmental Modelling & Software*, 146:105210, 2021.
- Shuangxi Miao, Shuyu Wang, Chunyan Huang, Xiaohong Xia, Lingling Sang, Jianxi Huang, Han Liu, Zheng Zhang, Junxiao Zhang, Xu Huang, et al. A big data grided organization and management method for cropland quality evaluation. *Land*, 12(10):1916, 2023.
- Colin PD Birch, Sander P Oom, and Jonathan A Beecham. Rectangular and hexagonal grids used for observation, experiment and simulation in ecology. *Ecological Modelling*, 206(3-4):347–359, 2007.
- Szymon Woźniak and Piotr Szymański. Hex2vec: Context-aware embedding H3 hexagons with OpenStreetMap tags. In *Proceedings of the 4th ACM SIGSPATIAL International Workshop on AI for Geographic Knowledge Discovery*, pages 61–71, 2021.
- Bing Han, Tengpeng Qu, Zili Huang, Qiangyu Wang, and Xinlong Pan. Emergency airport site selection using global subdivision grids. *Big Earth Data*, 6(3):276–293, 2022.
- Bing Han, Tengpeng Qu, Xiaochong Tong, Haipeng Wang, Hao Liu, Yuhao Huo, and Chengqi Cheng. AugGKG: A grid-augmented Geographic Knowledge Graph representation and spatio-temporal query model. *International Journal of Digital Earth*, 16(2):4934–4957, 2023.
- Benjamin Adams. Wāhi, a discrete global grid gazetteer built using linked open data. *International Journal of Digital Earth*, 10(5):490–503, 2017.
- David Habgood. RDFLib GeoSPARQL Functions for DGGS. URL <https://github.com/rdflib/geosparql-dggs>.
- Cogan Shimizu, Rui Zhu, Gengchen Mai, Colby Fisher, Ling Cai, Mark Schildhauer, Krzysztof Janowicz, Pascal Hitzler, Lu Zhou, and Shirly Stephen. A pattern for features on a hierarchical spatial grid. In *Proceedings of the 10th International Joint Conference on Knowledge Graphs*, pages 108–114, 2021.
- Dilshod Ibragimov, Katja Hose, Torben Bach Pedersen, and Esteban Zimányi. Optimizing aggregate SPARQL queries using materialized RDF views. In *The Semantic Web—ISWC 2016: 15th International Semantic Web Conference, Kobe, Japan, October 17–21, 2016, Proceedings, Part I 15*, pages 341–359. Springer, 2016.
- R de A Falbo, Giancarlo Guizzardi, Aldo Gangemi, and Valentina Presutti. Ontology patterns: clarifying concepts and terminology. In *Proceedings of the 4th Workshop on Ontology and Semantic Web Patterns*, volume 1188, 2013.
- Michael Lan, Xiaoying Wu, and Dimitri Theodoratos. Answering graph pattern queries using compact materialized views. In *DOLAP*, pages 51–60, 2022.
- Blake Regalia, Krzysztof Janowicz, and Song Gao. VOLT: A provenance-producing, transparent SPARQL proxy for the on-demand computation of linked data and its application to spatiotemporally dependent data. In *The Semantic Web. Latest Advances and New Domains: 13th International Conference, ESWC 2016, Heraklion, Crete, Greece, May 29–June 2, 2016, Proceedings 13*, pages 523–538. Springer, 2016.
- Sabine Timpf and Andrew U Frank. Using hierarchical spatial data structures for hierarchical spatial reasoning. In *Spatial Information Theory A Theoretical Basis for GIS: International Conference COSIT’97 Laurel Highlands, Pennsylvania, USA, October 15–18, 1997 Proceedings 3*, pages 69–83. Springer, 1997.

- Jedrzej Potoniec. Inductive learning of OWL 2 property chains. *IEEE Access*, 10:25327–25340, 2022.
- Eric J. Top. Understanding quantities in geo-information in terms of amounts, magnitudes, extents, and intents. pages 108–114, 2024.
- Emilie Stroh, Lars Harrie, and Susanna Gustafsson. A study of spatial resolution in pollution exposure modelling. *International journal of health geographics*, 6:1–13, 2007.
- W3C. Sparql 1.1 federated query, 2021. URL <https://www.w3.org/TR/sparql11-federated-query/>.
- Muhammad Saleem et al. Storage, indexing, query processing, and benchmarking in centralized and distributed RDF engines: a survey. *Authorea Preprints*, 2023.
- Li X Ren F and Geng D Thomson D. Geosharded Recommendations Part 1: Sharding Approach, 2018. URL <https://tech.gotinder.com/geosharded-recommendations-part-1-sharding-approach-2/>.
- Timo Homburg, Steffen Staab, and Daniel Janke. Geosparql+: Syntax, semantics and system for integrated querying of graph, raster and vector data. In *The Semantic Web–ISWC 2020: 19th International Semantic Web Conference, Athens, Greece, November 2–6, 2020, Proceedings, Part I* 19, pages 258–275. Springer, 2020.